Non-Biological Hierarchical Morphologies

Amphiphilic Molecules

Block Copolymers

Linear Polymer Static Chain Structure

Topological Polymers (Branched Chains, Gels and Networks, Cyclics)

Linear Polymer Dynamic Chain Structure

Polymer Crystalline Structure

Mass Fractal Aggregate Structure

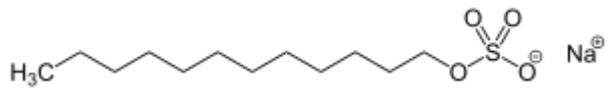

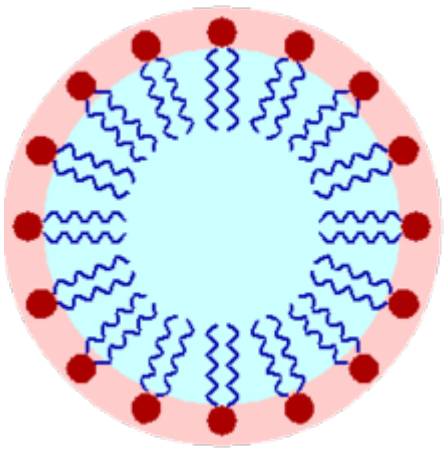

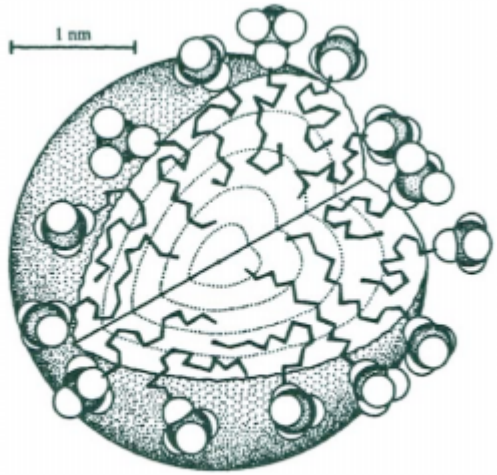

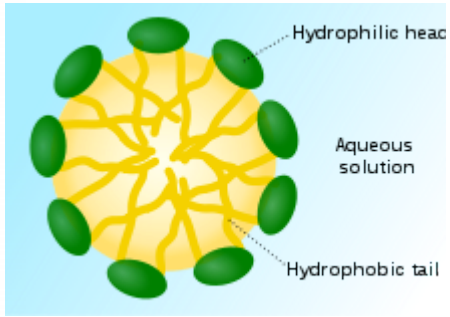

Figure 1. An illustration of a spherical micelle (for dodecyl sulphate) emphasizing the liquid like character with a disordered hydrocarbon core and a rough surface. (adapted from J. Israelachvili, Intermolecular and Surface Forces, Academic Press, London, 1985, p. 215)

http://www.eng.uc.edu/~gbeaucag/Classes/MorphologyofComplexMaterials/Amphiphilic.pdf

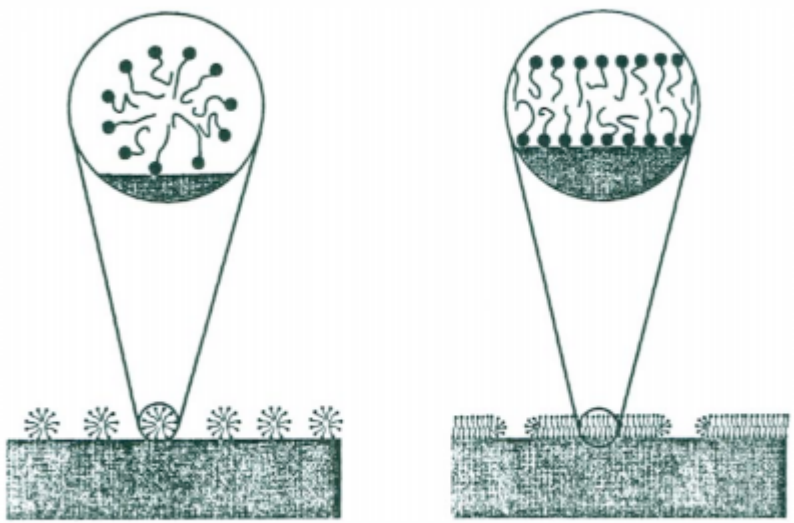

Figure 2. Surfactant molecules can self-assemble into discrete (spherical or cylindrical) micelles at a hydrophilic surface, in the absence of strong specific interactions between the surfactant head-group and the surface. (adapted from ref. [2], p. 60; © J. Wiley, 1998)

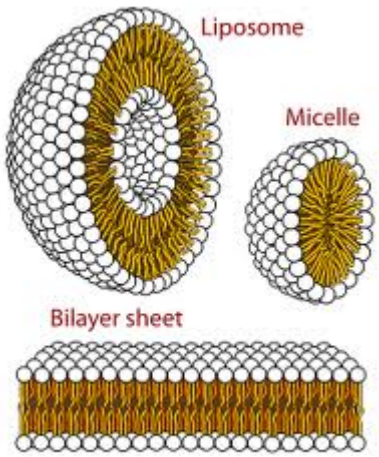

http://www.eng.uc.edu/~gbeaucag/Classes/MorphologyofComplexMaterials/Amphiphilic.pdf

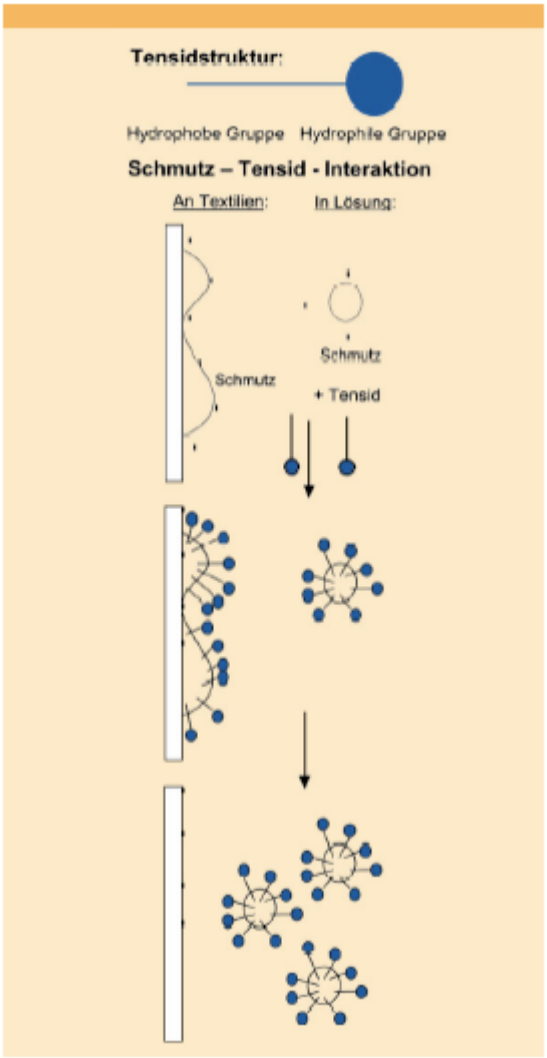

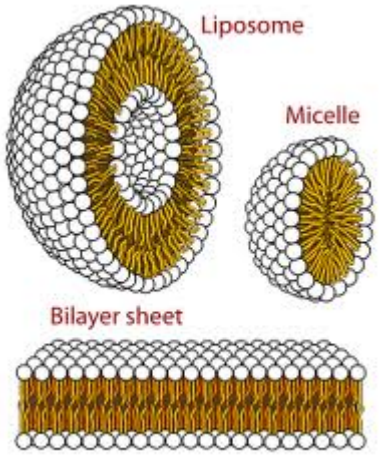

http://www.eng.uc.edu/~gbeaucag/Classes/MorphologyofComplexMaterials/Amphiphilic.pdf

http://www.mpikg.mpg.de/pdf/KolloidChemie/Scripte/Mizellbildung.pdf

Special preparation techniques necessary: „Cryo Transmission Electron microscopy“ (Cryo-TEM)

Micelle

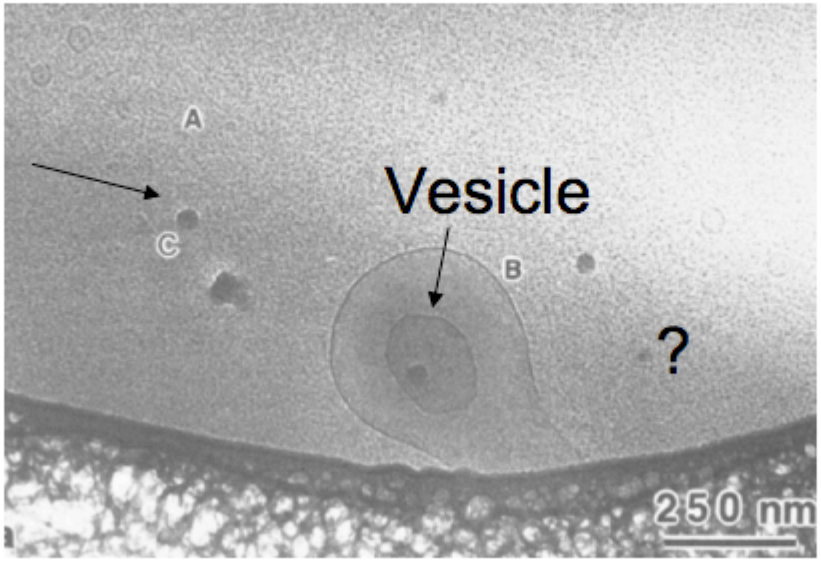

Evans, *Langmuir*, **1988**, *34*,1066.

http://www.eng.uc.edu/~gbeaucag/Classes/MorphologyofComplexMaterials/Amphiphilic.pdf

http://www.mpikg.mpg.de/pdf/KolloidChemie/Scripte/Mizellbildung.pdf

Visualization of self-assembled structures

Cylindrical micelles forming a stable 2D hexagonal lattice in a SiO_2 matrix

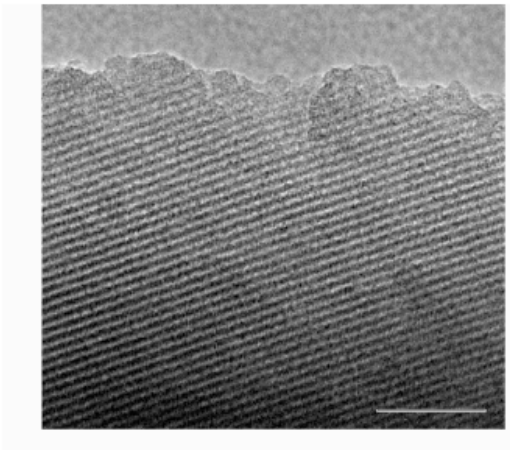

50 nm

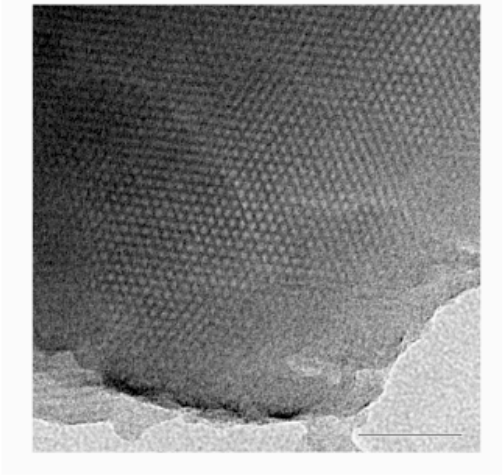

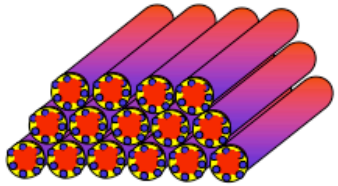

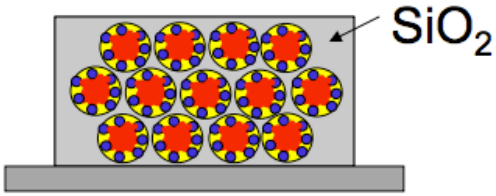

Pore structures can be seen as „cast“ of the micellar structure (Nanocasting)

MCM Catalyst system

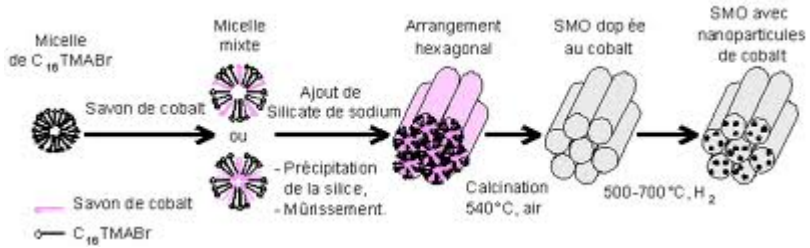

http://www.eng.uc.edu/~gbeaucag/Classes/MorphologyofComplexMaterials/Amphiphilic.pdf

http://www.mpikg.mpg.de/pdf/KolloidChemie/Scripte/Mizellbildung.pdf

The critical micelle concentration (cmc, c_k)

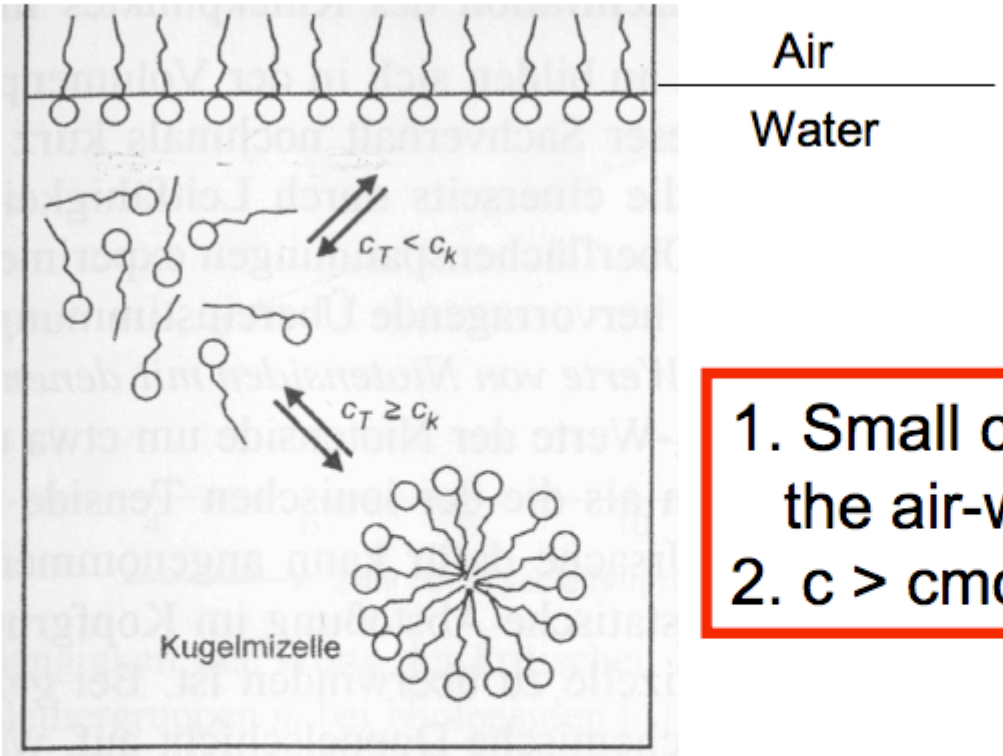

1. Small c: Adsorption of surfactants at the air-water interface
2. c > cmc : formation of micelles

cmc (c_k) = critical micelle concentration:

concentration, above which micelles are observed

$$\Delta G^\circ_{mic} = \mu^\circ_{mic} - \mu^\circ_{solv} = RT \ln (cmc)$$

http://www.eng.uc.edu/~gbeaucag/Classes/MorphologyofComplexMaterials/Amphiphilic.pdf

http://www.mpikg.mpg.de/pdf/KolloidChemie/Scripte/Mizellbildung.pdf

The critical micelle concentration (cmc, c_k)

Surface tension at cmc

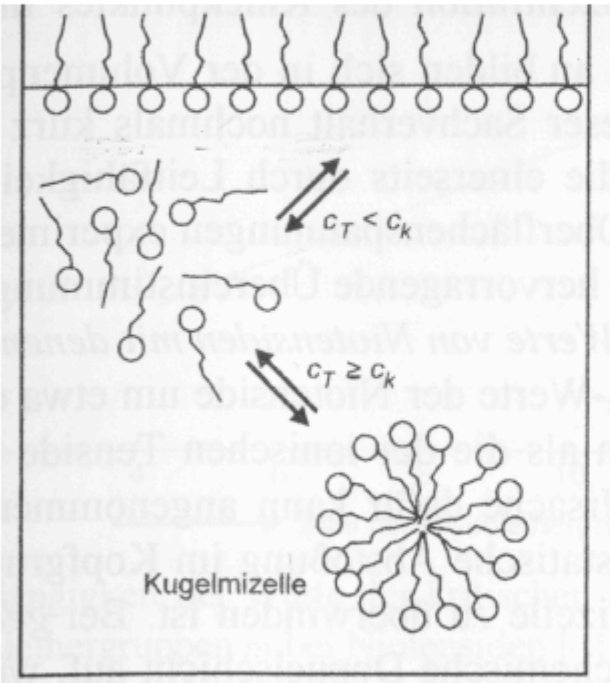

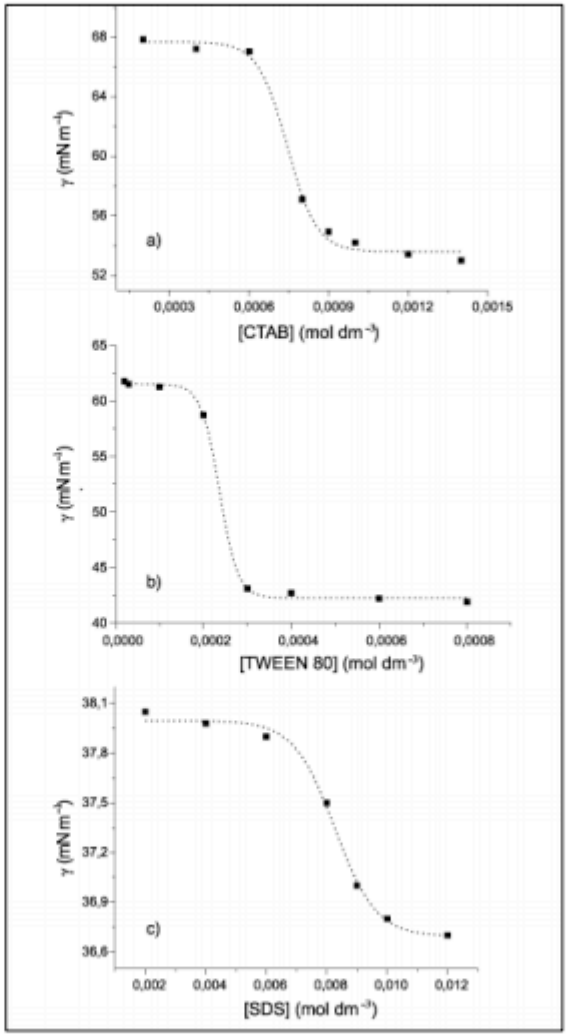

cmc of nonionic surfactants is generally lower compared to ionic surfactants

Abrupt changes at the cmc due to micelle formation!

http://www.eng.uc.edu/~gbeaucag/Classes/MorphologyofComplexMaterials/Amphiphilic.pdf

http://www.mpikg.mpg.de/pdf/KolloidChemie/Scripte/Mizellbildung.pdf

Summary: Some values about micelles

Micelle size:

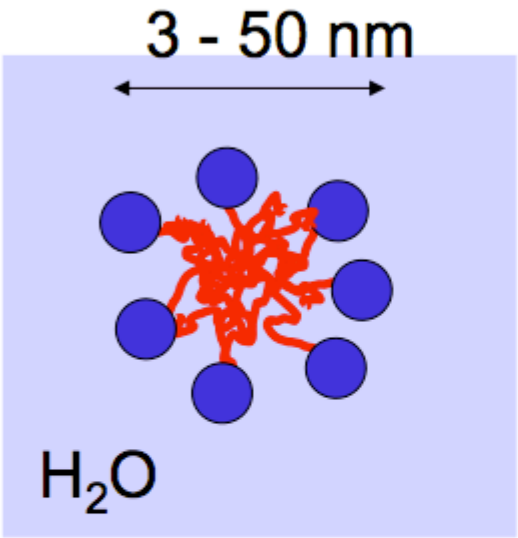

Aggregation number:

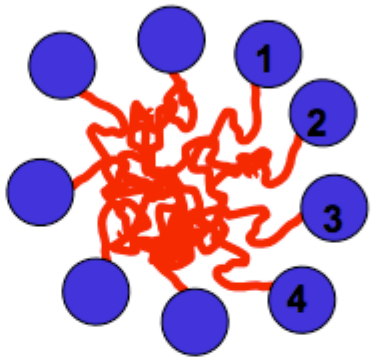

Ionic surfactants
z_A = 10-170

Nonionic surfactants
z_A = 30-10.000

Critical micelle concentrations (CMC):

cmc of ionic surfactants
is generally higher
compared to nonionic surfactants

Ionic surfactants
cmc = 10^{-3} – 10^{-2} M

Nonionic surfactants
cmc = 10^{-4} – 10^{-3} M

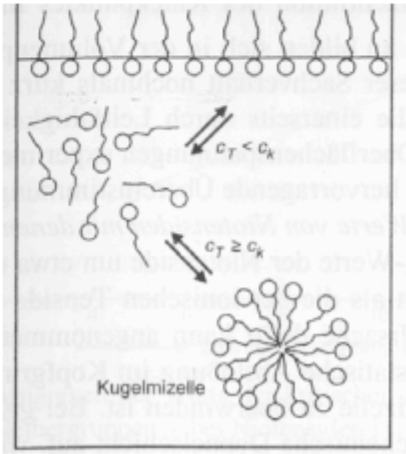

http://www.mpikg.mpg.de/pdf/KolloidChemie/Scripte/Mizellbildung.pdf

Solubility of surfactants-The Krafft temperature

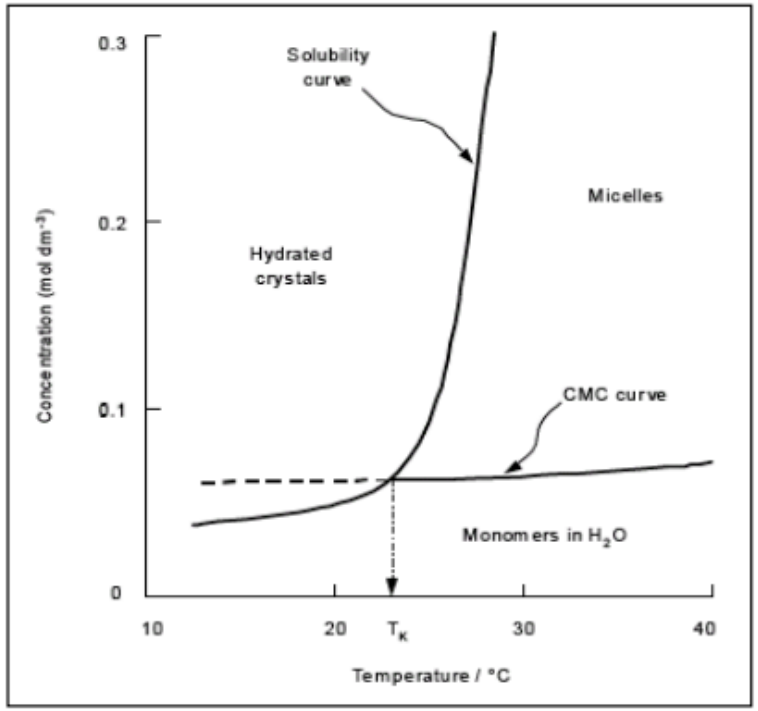

Binary phase diagram surfactant/water

- Solubility of surfactants highly T dependent
- Solubility is usually low at low T, rising rapidly in narrow range
- No micelles possible above a certain temperature
- The point where solubility curve meets CMC curve is the Krafft point, which defines the T_{krafft}..
- The Krafft temperature can be regarded as a „melting point“

http://www.eng.uc.edu/~gbeaucag/Classes/MorphologyofComplexMaterials/Amphiphilic.pdf

http://www.mpikg.mpg.de/pdf/KolloidChemie/Scripte/Mizellbildung.pdf

The concept of the "packing parameter P" (Israelachvili, 1976)

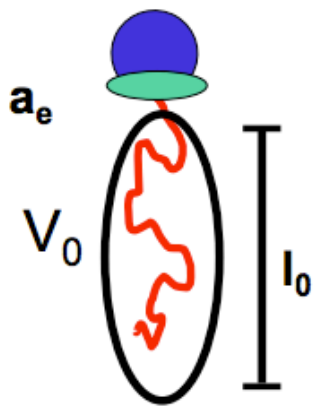

$$P = V_0/(a_e\, l_0)$$

V_0 **surfactant tail volume**

a_e ***equilibrium*** **area per molecule at the aggregate interface**

l_0 **tail length**

Common surfactants:
v_0/l_0 = const. = 0.21 nm² (single tail)

Example: Spherical micelle with aggregation number g

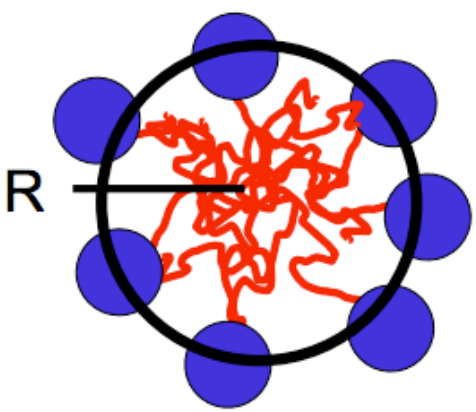

$$\left.\begin{aligned} V_{core} &= g\, V_0 = 4\pi R^3/3 \\ A &= g\, a_e = 4\pi R^2 \end{aligned}\right\} \quad R = 3\, V_0/a_e$$

With $R \le l_0$ ⇒ $0 \le V_0/(a_e\, l_0) \le 1/3$

http://www.eng.uc.edu/~gbeaucag/Classes/MorphologyofComplexMaterials/Amphiphilic.pdf

http://www.mpikg.mpg.de/pdf/KolloidChemie/Scripte/Mizellbildung.pdf

The concept of the "packing parameter P" (Israelachvili)

Table 2.1 Expected aggregate characteristics in relation to surfactant critical packing parameter, $P_c = v/a_0 l_c$

P_c	General Surfactant type	Expected Aggregate Structure
< 0.33	Single-chain surfactants with large head groups	Spherical or ellipsoidal micelles
0.33 - 0.5	Single-chain surfactants with small head groups, or ionics in the presence of large amounts of electrolyte	Large cylindrical or rod-shaped micelles Vesicles and flexible bilayers structures
0.5 - 1.0	Double-chain surfactants with large head groups and flexible chains	Planar extended bilayers
1.0	Double-chain surfactants with small head groups or rigid, immobile chains	Reversed or inverted micelles
>1.0	Double-chain surfactants with small head groups, very large and bulky hydrophobic groups	

Figure 2.6 Changes in the critical packing parameters (P_c) of surfactant molecules give rise to different aggregation structures.

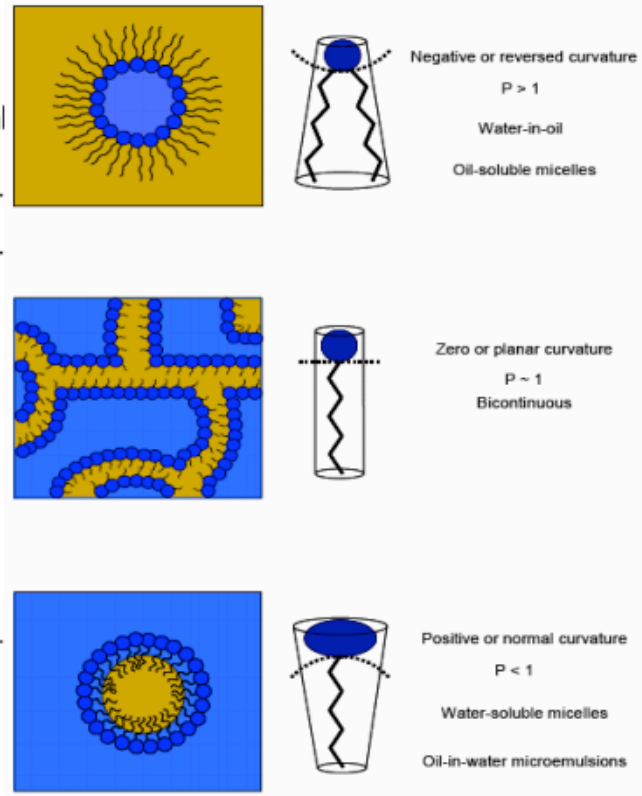

http://www.eng.uc.edu/~gbeaucag/Classes/MorphologyofComplexMaterials/Amphiphilic.pdf

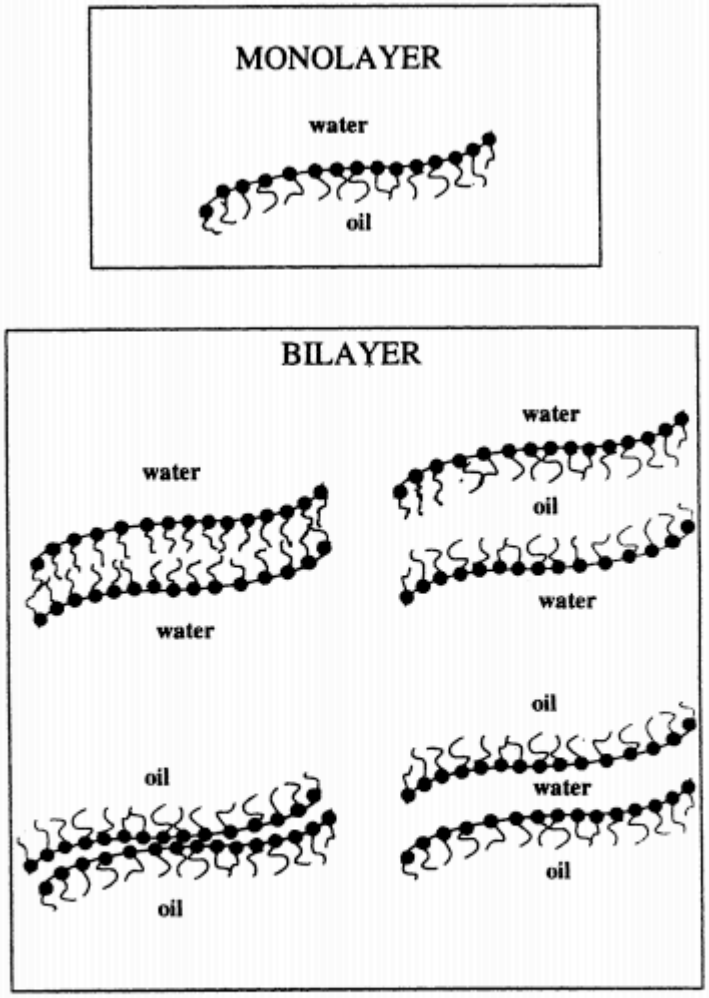

Figure 3. Surfactant monolayer (top panel) and bilayers (bottom panel). In any surfactant system we have a segregation into water-rich and oil-rich domains, as well as surfactant films. The latter can be pairwise correlated (into bilayers) or uncorrelated. (adapted from D.O. Shah, Ed., Micelles, Microemulsions, and Monolayers, Marcel Dekker, 1998, p. 105)

http://www.eng.uc.edu/~gbeaucag/Classes/MorphologyofComplexMaterials/Amphiphilic.pdf

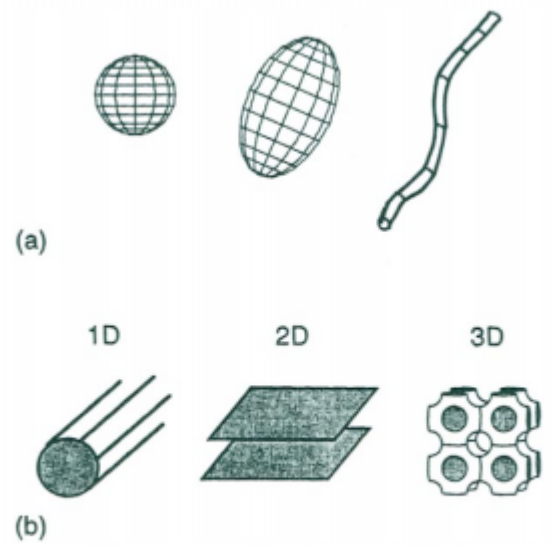

Figure 4. Examples of (a) discrete and (b) continuous surfactant self-assemblies. The latter can extend on 1 (cylinders), 2 (lamellae) or 3 (bicontinuous) dimensions. (adapted from D. O. Shah, Ed., Micelles, Microemulsions, and Monolayers, Marcel Dekker, 1998, p. 104)

http://www.eng.uc.edu/~gbeaucag/Classes/MorphologyofComplexMaterials/Amphiphilic.pdf

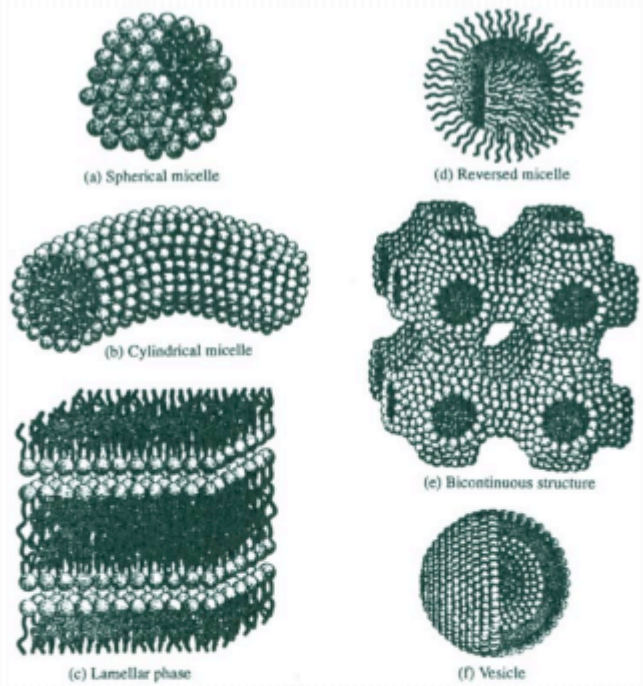

Figure 5. Surfactant self-assembly leads to a range of different structures of which a few are shown: (a) Spherical micelle with an interior composed of the hydrocarbon chains and a surface of the polar head-groups (depicted as spheres) facing water. The hydrocarbon core has a radius close to the length of the extended alkyl chain. (b) Cylindrical micelle with an interior composed of the hydrocarbon chains and a surface of the polar head-groups facing water. The cross section of the hydrocarbon core is similar to that of spherical micelles. The micellar length is highly variable so these micelles are polydisperse. (c) Lamellar phase consisting of surfactant bilayers. (d) Reverse micelle with a water core surrounded by the surfactant polar head-groups. The alkyl chains together with a non-polar solvent make up the continuous medium. (e) Bicontinuous structure with the surfactant molecules assembled into connected films characterized of two curvatures of opposite sign. (f) Vesicle built from bilayers similar to those of the lamellar phase, and characterized by two distinct aqueous domains, one forming the core and one the external medium. (adapted from ref. [2], p. 34; © J. Wiley, 1998)

http://www.eng.uc.edu/~gbeaucag/Classes/MorphologyofComplexMaterials/Amphiphilic.pdf

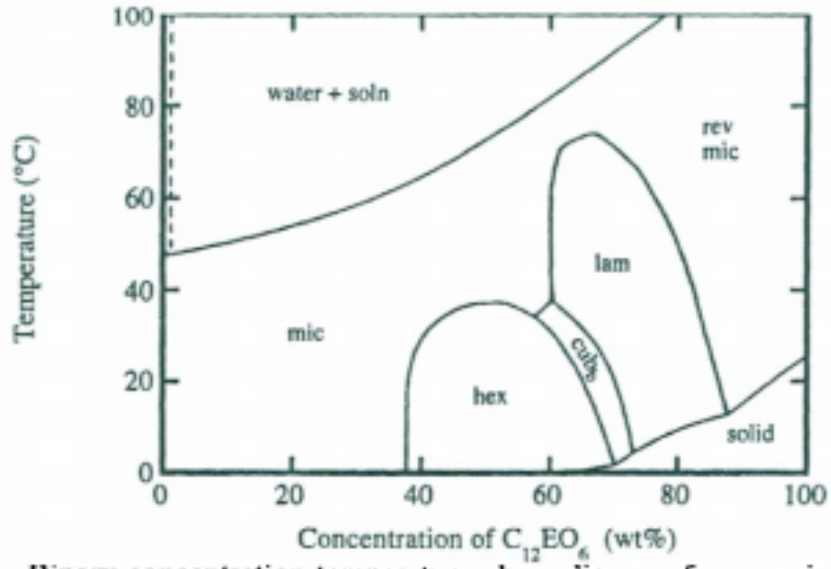

Figure 6. Binary concentration-temperature phase diagram for a nonionic surfactant with C12 hydrophobic chain and 6 oxyethylenes in the polar head group. Mic and rev mic denote micellar and reverse micellar solutions, respectively. Hex, cub, and lam, denote regions with hexagonal, cubic, and lamellar lyotropic liquid crystalline microstructure, respectively. (adapted from ref. [2], p. 99; © J. Wiley, 1998)

http://www.eng.uc.edu/~gbeaucag/Classes/MorphologyofComplexMaterials/Amphiphilic.pdf

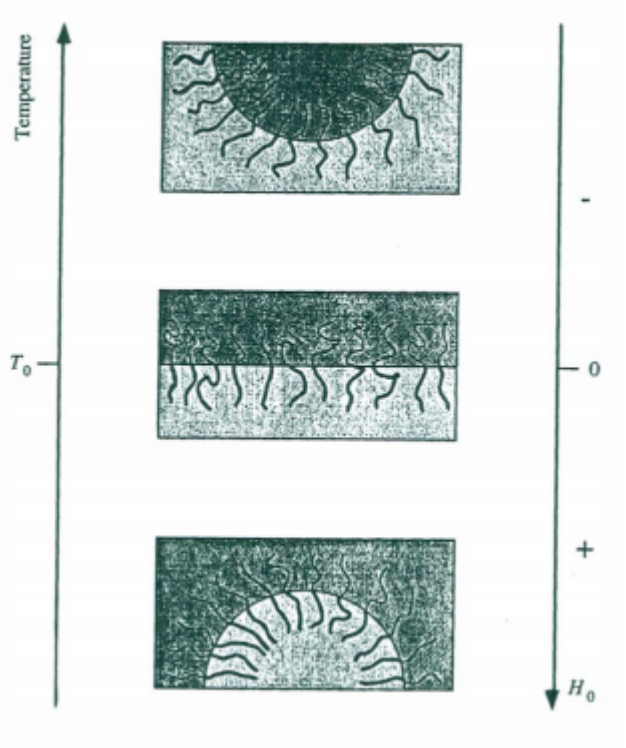

http://www.eng.uc.edu/~gbeaucag/Classes/MorphologyofComplexMaterials/Amphiphilic.pdf

Block Copolymers

http://www.eng.uc.edu/~gbeaucag/Classes/MorphologyofComplexMaterials/BCP%20Section.pdf

Block Copolymers

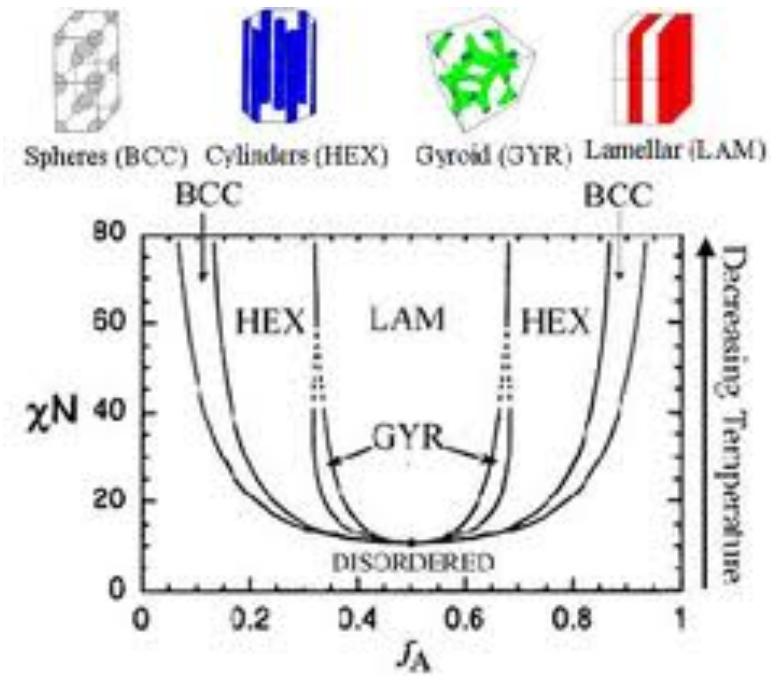

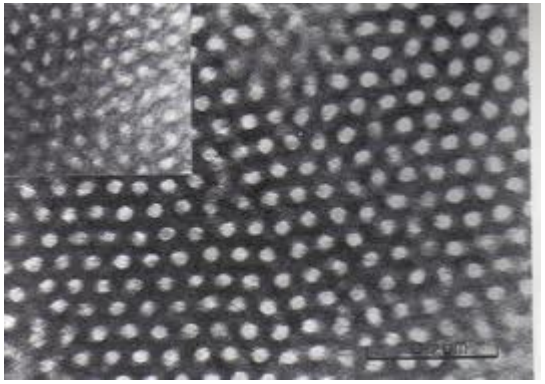

SBR Rubber

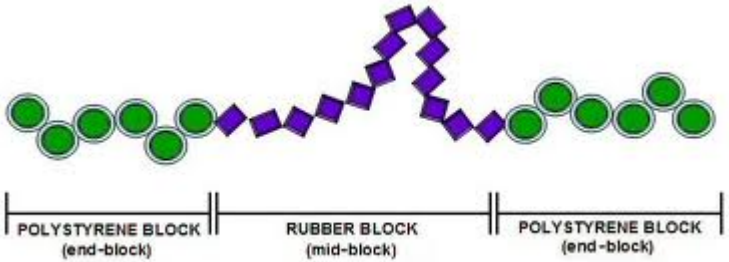

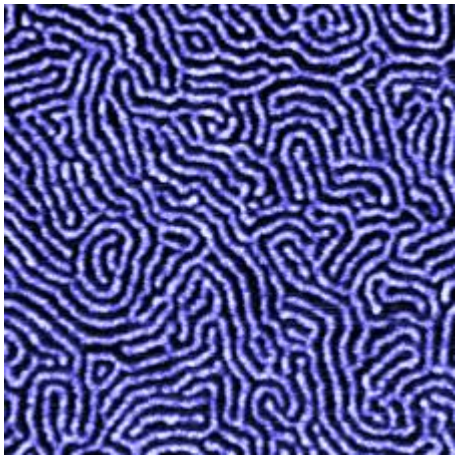

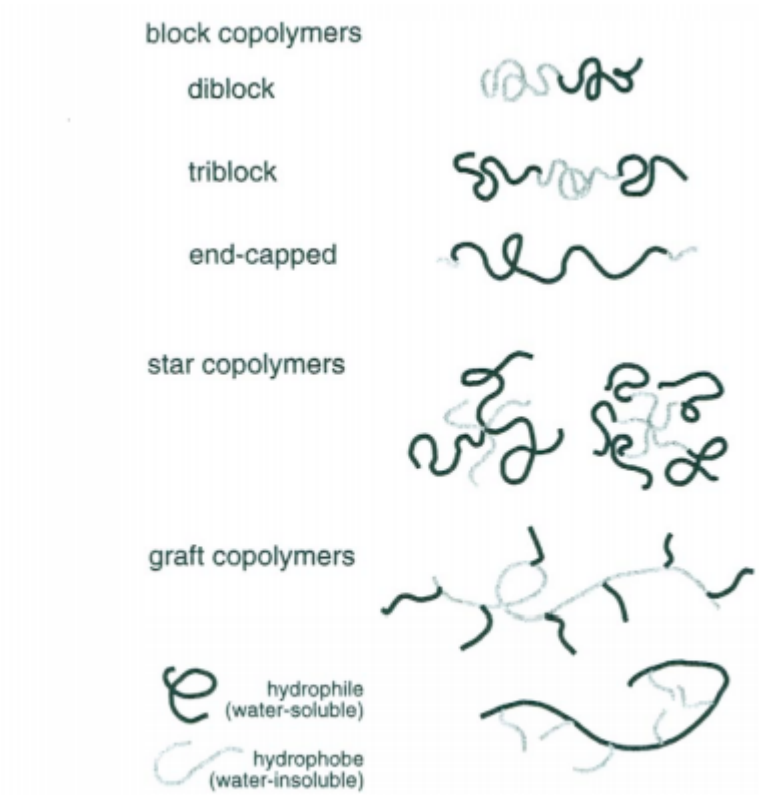

Figure 9. Schematics of block, star, and graft amphiphilic block copolymers.

http://www.eng.uc.edu/~gbeaucag/Classes/MorphologyofComplexMaterials/Amphiphilic.pdf

16

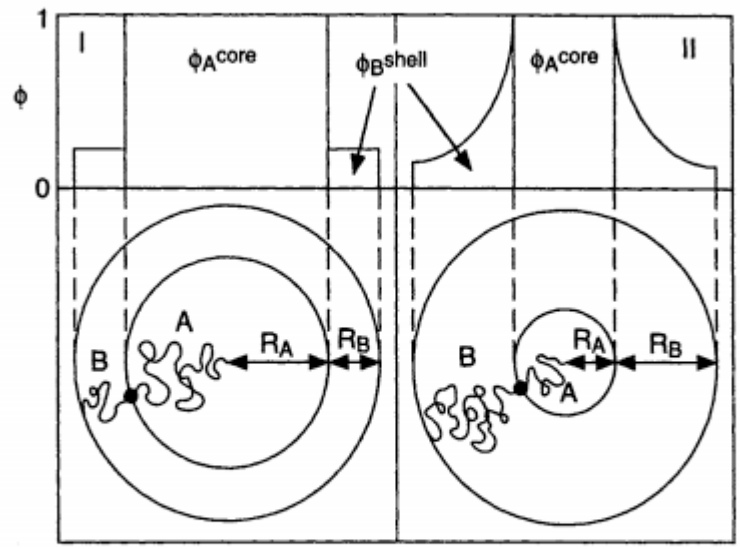

Figure 1. Illustration of model I (left) and II (right) of the AB-diblock copolymer micelle in a selective solvent (lower panel) and the volume fraction profiles of the polymer blocks (upper panel) applied for the large core case ($N_A >> N_B$) and the small core case ($N_A << N_B$), respectively.

http://www.eng.uc.edu/~gbeaucag/Classes/MorphologyofComplexMaterials/BCP%20Modeling.pdf

Hierarchy in BCP's and Micellar Systems

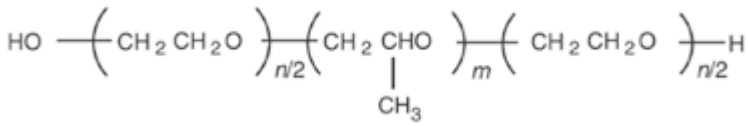

Pluronics (PEO/PPO block copolymers)

We consider primary structure as the block nature of the polymer chain.

This is similar to hydrophobic and hydrophilic interactions in proteins.

These cause a secondary self-organization into rods/spheres/sheets.

A tertiary organizaiton of these secondary structures occurs.

There are some similarities to proteins but BCP's are extremely simple systems by comparison.

What is the size of a Block Copolymer Domain?

Masao Doi, Introduction to Polymer Physics

-For and symmetric A-B block copolymer
-Consider a lamellar structure with Φ = 1/2
-Layer thickness D in a cube of edge length L, surface energy σ
- $F_{surface} \cong 2\sigma \frac{L}{D} L^2$ so larger D means less surface and a lower Free Energy F.
-The polymer chain is stretched as D increases. The free energy of a stretched chain as a function of the extension length D is given by

- $F_{stretch} \cong kT \frac{D^2}{Nb^2} \frac{L^3}{N\upsilon_c}$ where N is the degree of polymerization for A or B,

b is the step length per N unit, νc is the excluded volume for a unit step
So the stretching free energy, F, increases with D^2.

-To minimize the free energies we have $D \cong \left(\frac{\sigma N^2 b^2 \upsilon_c}{kT} \right)^{1/3} \sim N^{2/3}$

Synthetic Polymer Chain Structure
(A Statistical Hierarchy)

Random Walk Generator (Manias Penn State)

http://zeus.plmsc.psu.edu/~manias/MatSE443/Study/7.html

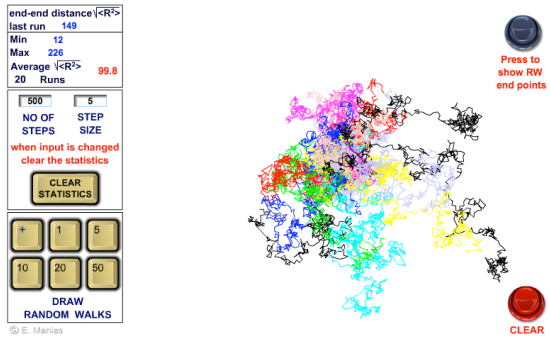

(-This simulation will probably lead to Guinier's Law)

-Polymers do not have a discrete size, shape or conformation.

-Looking at a single simulation of a polymer chain is of no use.

-We need to consider average features.

-Every feature of a polymer is subject to a statistical description.

-Scattering is a useful technique to quantify a polymer since it describes structure from a statistically averaged perspective as we have seen previously (Guinier's Law for instance).

Chain Scaling (Long-Range Interactions)

Long-range interactions are interactions of chain units separated by such a great index difference that we have no means to determine if they are from the same chain other than following the chain over great distances to determine the connectivity. That is, Orientation/continuity or polarity and other short range linking properties are completely lost.

Long-range interactions occur over short spatial distances (as do all interactions).

Consider chain scaling with no long-range interactions.

The chain is composed of a series of steps with no orientational relationship to each other.

So <R> = 0

<R^2> has a value:

$$\left\langle R^2 \right\rangle = \sum_i \sum_j r_i \bullet r_j = \sum_i r_i \bullet r_i + \sum_i \sum_{j \neq i} r_i \bullet r_j$$

We assume no long range interactions so that the second term can be 0.

$$\left\langle R^2 \right\rangle = Nr^2$$

The Primary Structure for Synthetic Polymers

Worm-like Chain
Freely Jointed Chain
Freely Rotating Chain
Rotational Isomeric State Model Chain (RISM)
Persistent Chain
Kuhn Chain

These refer to the local state of the polymer chain.

Generally the chain is composed of chemical bonds
that are directional, that is they are rods connected at their ends.

These chemical steps combine to make an effective
rod-like base unit, the persistence length,
for any synthetic polymer chain (this is larger than the chemical step).

The persistence length can be measured in scattering
or can be inferred from rheology through the Kuhn length

$$l_K = 2\, l_P$$

The Primary Structure for Synthetic Polymers

Short-Range Interactions

The persistence length is created due to interactions between units of the chain that have similar chain indicies

These interactions are termed "short-range interactions" because they involve short distances along the chain path

Short-range interactions lead to changes in the chain persistence. For example, restrictions to bond rotation such as by the addition of short branches can lead to increases in the persistence length in polymers like polyethylene. Short-range interactions can be more subtle. For instance short branches in a polyester can disrupt a natural tendency to form a helix leading to a reduction in the persistence length, that is making the chain more flexible.

All interactions occur over short spatial distances, short-range interactions occur over short-distances but the distinguishing feature is that they occur over short differences in chain index.

Short-range interactions do not have an effect on the chain scaling.

The Primary Structure for Synthetic Polymers

Scattering Observation of the Persistence Length

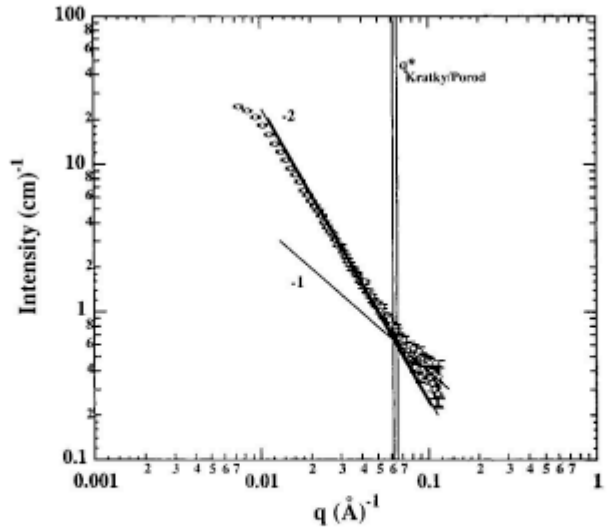

Figure 2. *Kratky/Porod graphical analysis in a log-log plot of corrected SANS data from a 5% by volume d-PHB sample in h-PHB. The lower power -2 line is the best visual estimate; the upper line is shifted to match a global unified fit. Key: left, q* corresponds to best visual estimate; right, plot to match global unified fit. The statistical error in the data is shown [3].*

A power-law decay of -1 slope has only one structural interpretation.

The Primary Structure for Synthetic Polymers

Consider a Brownian path with an index or continuous postion variable "s". For the simulated walks "s" is the time. For a polymer chain "s" is the chain index. Next consider an arbitrary origin of a coordinate system (0,0,0) and vectors to positions of the walk **r**(s). The unit tangent vector to the walk, **t**(s), is defined by,

$$\bar{t}(s) = \frac{\partial \bar{r}(s)}{\partial s} \quad (1)$$

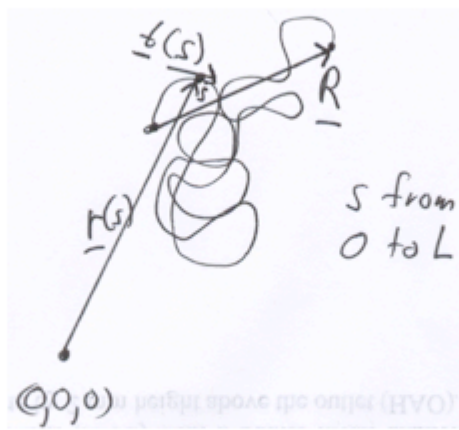

Figure 1. Brownian Path.

The end-to-end distance for the Brownian path is given by,

$$\bar{R} = \int_0^L \bar{t}(s)\,ds \quad (2)$$

The auto-correlation function for the tangent vector can be written,

$$\langle t(s) \bullet t(0) \rangle = e^{-s/l_p} \quad (3)$$

if a linear decay in correlation can be assumed. That is,

$$d(\langle t(s) \bullet t(0) \rangle) = -\langle t(s) \bullet t(0) \rangle \left(\frac{1}{l_p} \right) ds \quad (4)$$

The persistence length is then similar to the linear absorption coefficient for radiation.

(2) and (3) can be used to calculate the mean square end-to-end distance $\underline{R}^2$,

$$\langle R^2 \rangle = \langle \overline{R} \bullet \overline{R} \rangle = \left\langle \int_0^L \bar{t}(s) ds \bullet \int_0^L \bar{t}(s') ds' \right\rangle = \int_0^L \left(ds \int_0^L \langle \bar{t}(s) \bullet \bar{t}(s') \rangle ds' \right) = \int_0^L \left(ds \int_0^L \exp\left(\frac{-|s-s'|}{l_p} \right) ds' \right)$$

$$= 2l_p L \left(1 - \frac{l_p}{L} \left(1 - e^{-L/l_p} \right) \right) \cong 2l_p L$$

We also can consider that for a freely jointed chain composed of n_K Kuhn steps of length l_K,

$$\langle R^2 \rangle = n_K l_K^2 = l_K L = 2 l_p L$$

Showing that the freely jointed Kuhn length is just twice the persistence length.

The Secondary Structure for Synthetic Polymers
Long-Range Interactions

Boltzman Probability
For a Thermally Equilibrated System

$$P_B(R) = \exp\left(-\frac{E(R)}{kT}\right)$$

Gaussian Probability
For a Chain of End to End Distance R

$$P(R) = \left(\frac{3}{2\pi\sigma^2}\right)^{3/2} \exp\left(-\frac{3(R)^2}{2(\sigma)^2}\right)$$

By Comparison The Energy to stretch a Thermally Equilibrated Chain Can be Written

$$E = kT\frac{3R^2}{2nl_K^2}$$

For a Chain with Long-Range Interactions There is and Additional Term

$$P_{Ex}(R) = \left(1 - V_c/R^3\right)^{n^2/2} = \exp\left(\frac{n^2 \ln\left(1 - V_c/R^3\right)}{2}\right) \sim \exp\left(-\frac{n^2 V_c}{2R^3}\right)$$

So,

$$E = kT\left(\frac{3R^2}{2nl_K^2} + \frac{n^2 V_c}{2R^3}\right)$$

Finding the Minimum Energy at dE/dR = 0 Yields: $R^* \sim l_K\, n^{3/5}$

Flory-Krigbaum Theory
Result is called a Self-Avoiding Walk

The Secondary Structure for Synthetic Polymers

Linear Polymer Chains have Two Possible Secondary Structure States:

Self-Avoiding Walk	Gaussian Chain
Good Solvent	Random Walk
Expanded Coil	Theta-Condition
(The Normal Condition in Solution)	Brownian Chain
	Flory Radius R_F
	(The Normal Condition in the Melt/Solid)
$R^* \sim l_K\, n^{3/5}$	$\langle R^2 \rangle = Nl^2$
$d_f = 5/3 \approx 1.67$	$d_f = 2$

These are statistical features. That is, a single simulation of a SAW and a GC could look identical.

The Secondary Structure for Synthetic Polymers

Linear Polymer Chains have Two Possible Secondary Structure States:

Self-Avoiding Walk	Gaussian Chain
Good Solvent	Random Walk
Expanded Coil	Theta-Condition
(The Normal Condition in Solution)	Brownian Chain
	(The Normal Condition in the Melt/Solid)
$R^* \sim l_K\, n^{3/5}$	$\langle R^2 \rangle = Nl^2$
$d_f = 5/3 \approx 1.67$	$d_f = 2$

Consider going from dilute conditions, c < c*, to the melt by increasing concentration.
The transition in chain size is gradual not discrete.
Synthetic polymers at thermal equilibrium accommodate concentration changes through a scaling transition. Primary, Secondary, Tertiary Structures.

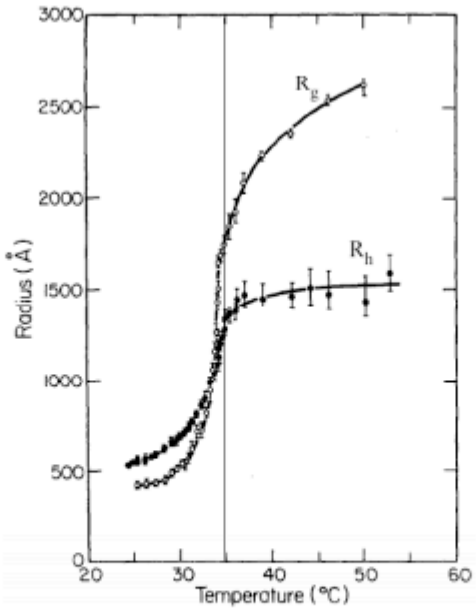

Figure 3. *Radius of gyration, R_g, and hydrodyamic radius R_h versus temperature for polystyrene in cyclohexane. Vertical line indicates the phase separation temperature. From Reference [21].*

For a polymer in solution there is an inherent concentration to the chain since the chain contains some solvent

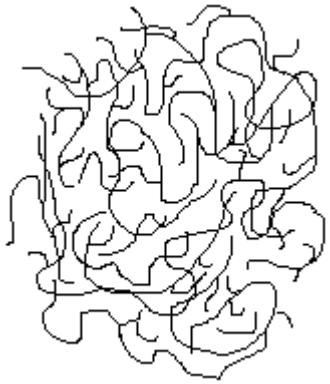

The polymer concentration is Mass/Volume, within a chain

$$c^* = \frac{Mass}{Volume} = \frac{Mass}{Size^3} = \frac{Size^{d_f}}{Size^3} \sim Size^{d_f - 3}$$

$$c^* \sim n^{\left(1 - 3/d_f\right)}$$

When the solution concentration matches c* the chains "overlap"
Then an individual chain is can not be resolved and the chains entangle
This is called a concentrated solution, the regime near c* is called semi-dilute
and the regime below c* is called dilute

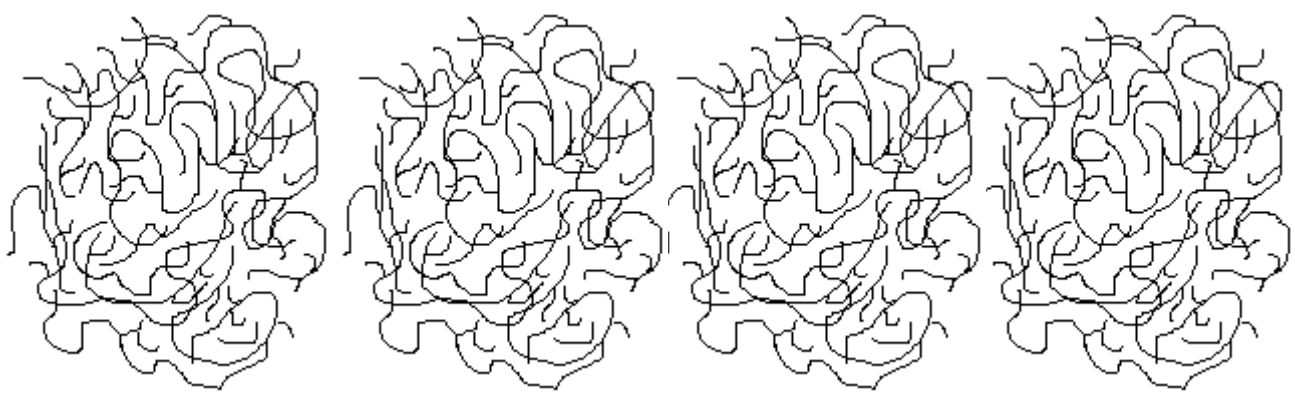

In concentrated solutions with chain overlap chain entanglements lead to a higher solution viscosity

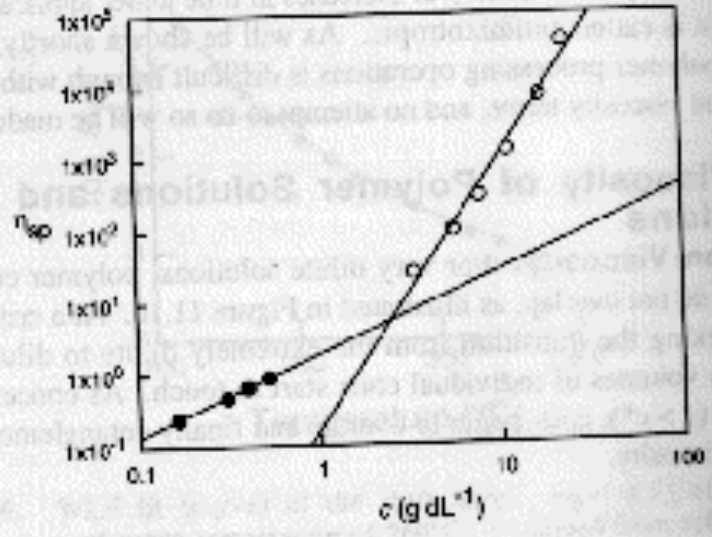

Figure 11.17. Concentration dependence of the specific viscosity of dilute and moderately concentrated solutions of cellulose acetate in dimethyl sulfoxide.[3] The intersection of straight lines that are drawn through the dilute-solution (●) and concentrated-solution (○) data marks the critical concentration, c^* (ca. 3.7 g dL^{-1} in this case).

J.R. Fried Introduction to Polymer Science

$$\eta \sim c^P$$

$$P = 1 \text{ for c} < \text{c*}$$

In dilute solution the coil contains a concentration $c^* \sim 1/[\eta]$

$$c^* = k\, n/R^3 = k\, n^{-4/5}$$ for good solvent conditions

At large sizes the coil acts as if it were in a concentrated solution, df = 2. At small sizes the coil acts as if it were in a dilute solution, df = 5/3. There is a size scale, ξ, where this "scaling transition" occurs.

We have a primary structure of rod-like units, a secondary structure of expanded coil and a tertiary structure of Gaussian Chains.

What is the value of ξ?

ξ is related to the coil size R since it has a limiting value of R for $c < c^*$ and has a scaling relationship with the reduced concentration c/c^*

$$\xi \sim R\,(c/c^*)^P \sim n^{(3+4P)/5}$$

There are no dependencies on n above c^* so $(3+4P)/5 = 0$ and $P = -3/4$

$$\xi \sim R\,(c/c^*)^{-3/4}$$

In terms of the Flory Radius

$$R = \xi\, n_{\xi}^{1/2} = R_{F0}\,(c/c^*)^{-3/4}\,(c/c^*)^{5/8} = R_{F0}\,(c/c^*)^{-1/8}$$

This is called the "Concentration Blob"

Tensile Blob

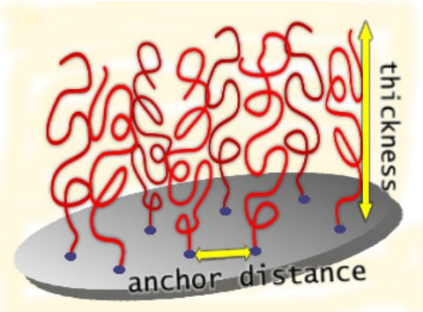

$$E = kT\frac{3R^2}{2nl_K^2} \qquad F = \frac{dE}{dR} = \frac{3kT}{nl_K^2}R$$

For weak perturbations of the chain $R \approx n^{1/2} l_K \equiv \xi_{Tensile}$

$$\xi_{Tensile} = \frac{3kT}{F}$$

Application of an external stress to the ends of a chain create a transition size where the coil goes from Gaussian to Linear called the Tensile Blob.

Thermal Blob

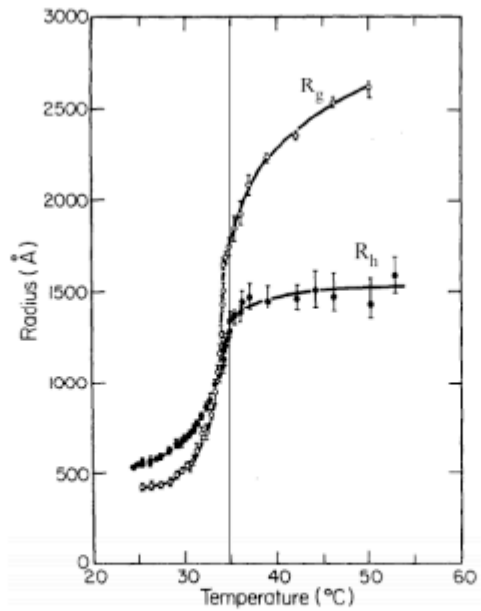

Figure 3. *Radius of gyration, R_g, and hydrodyamic radius R_h versus temperature for polystyrene in cyclohexane. Vertical line indicates the phase separation temperature. From Reference [21].*

Chain expands from the theta condition to fully expanded gradually.
At small scales it is Gaussian, at large scales expanded (opposite of concentration blob).

$$E = kT\left(\frac{3R^2}{2nl_K^2} + \frac{n^2V_c}{2R^3}\right)$$

$$E = kT\left(\frac{3R^2}{2nl_K^2} + \frac{n^2V_c(1-2\chi)}{2R^3}\right)$$

Thermal Blob

$$\Delta\varepsilon = \left(\varepsilon_{PP} + \varepsilon_{SS}\right)/2 - \varepsilon_{PS}$$

$$\chi = \frac{z\Delta\varepsilon}{kT}$$

$$V_{c,enthalpic} = V_c\left(1 - 2\chi\right)$$

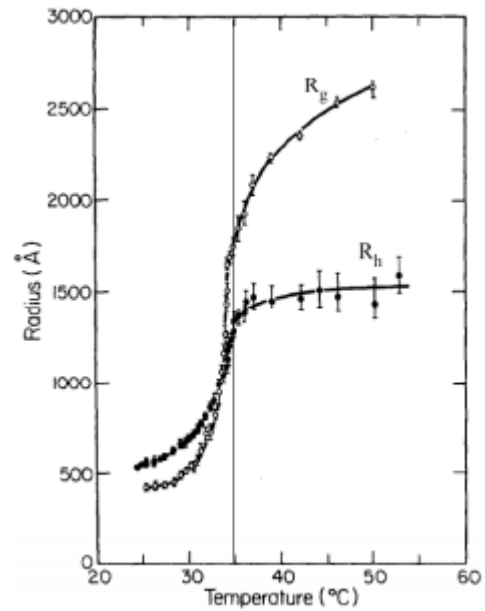

$$E = kT\left(\frac{3R^2}{2nl_K^2} + \frac{n^2V_c}{2R^3}\right)$$

$$E = kT\left(\frac{3R^2}{2nl_K^2} + \frac{n^2V_c\left(1-2\chi\right)}{2R^3}\right)$$

Thermal Blob

$$E = kT\left(\frac{3R^2}{2nl_K^2} + \frac{n^2V_c(1-2\chi)}{2R^3}\right)$$

Energy Depends on n, a chain with a mer unit of length 1 and n = 10000
could be re cast (renormalized) as a chain of unit length 100 and n = 100
The energy changes with n so depends on the definition of the base unit

Smaller chain segments have less entropy so phase separate first.
We expect the chain to become Gaussian on small scales first.
This is the opposite of the concentration blob.

Cooling an expanded coil leads to local chain structure collapsing to a Gaussian structure first.
As the temperature drops further the Gaussian blob becomes larger until the entire chain is Gaussian at the theta temperature.

Thermal Blob

$$R = N_T^{3/5}\xi_T = \left(N/n_T\right)^{3/5}\xi_T = \left(N\Big/\left(\xi_T/l\right)^2\right)^{3/5}\xi_T = N^{3/5}\xi_T^{-1/5}l^{6/5}$$

Flory-Krigbaum Theory yields: $R = V_c^{1/5}\left(1-2\chi\right)^{1/5}N^{3/5}l^{2/5}$

By equating these:

$$\xi_T = \frac{l}{\left(1-2\chi\right)}$$

Fractal Aggregates and Agglomerates

Growth of Nanoparticles

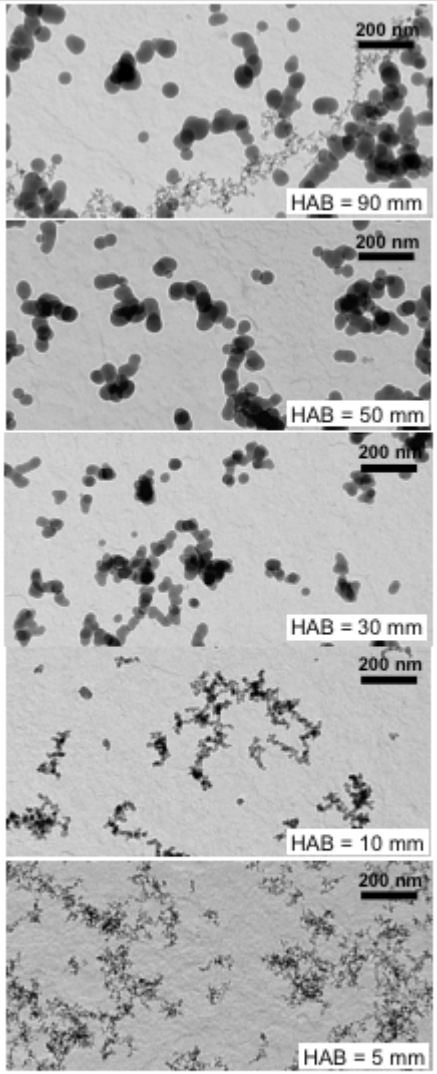

Fig. 1: Silica particles as collected by conventional thermophoretic sampling (TS) along the axis of a premixed flame of hexamethyldisiloxane and oxygen [1,2]. Using aluminum foil in-stead of TEM grids and performing multiple sampling from the same location in the flame, the Al-probe was covered with ***a silica monolayer*** *[1] (as indicated in Fig. 2).*

Spray Flame Appearance

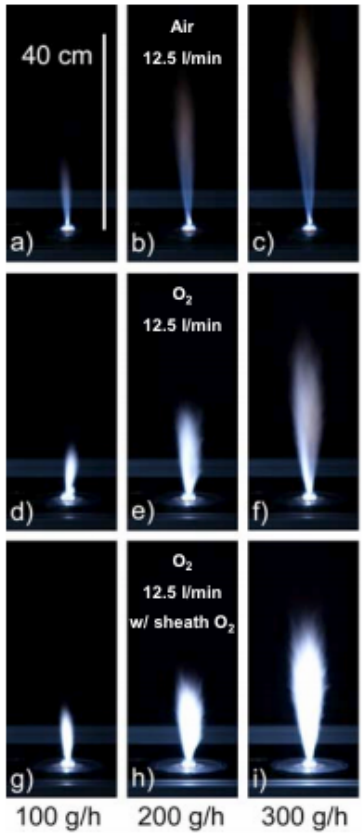

Fig. 3: Spray flames (1.26 M HMDSO in EtOH) producing 100, 200 and 300 g/h of silica using 12.5 l/min air (a-c) or O_2 as dispersion gas without (d-f) and with (g-i) additional 25 l/min of O_2 sheath flow at 1 bar pressure drop across the nozzle tip.

Powder Morphology

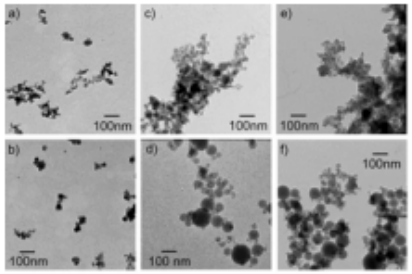

Fig. 4: Transmission electron micrographs of silica nanoparticles at production rates of 150 (top row) and 300 g/h (bottom row) using 12.5 l/min air (a,b) or O_2 as dispersion gas without (c,d) and with (e,f) additional 25 l/min of O_2 sheath flow using 1.26 M HMDSO in EtOH.

Powder Morphology

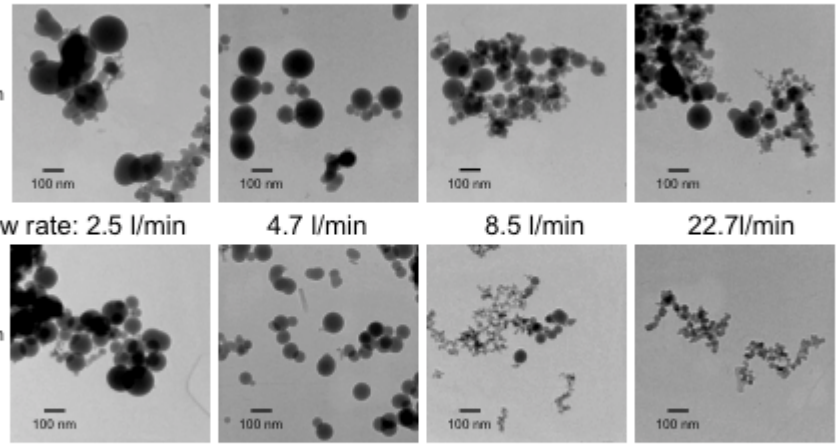

Fig. 5: Transmission Electron Micrographs (TEM) of SiO_2 synthesized in SDF and DDF at different oxygen flow rates. Particles made in flames at low oxygen flow rates stay longer at high temperatures leading to the formation of rather big spherical, non-agglomerated particles with diameters of about 100 nm. At high oxygen flow rates the particles are agglomerates of small primary particles. Particles synthesized in DDF have narrower size distributions indicated by TEM compared to those made in SDF.

Flame Structure

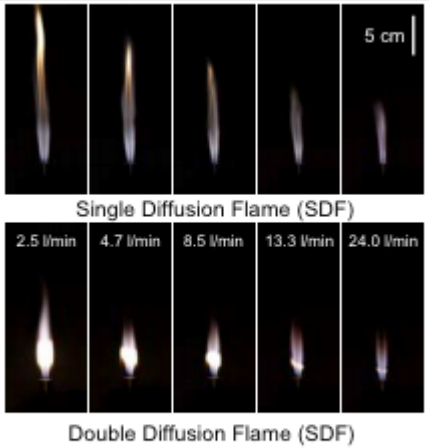

Fig. 3: Effect of oxygen flow rate on flame structure of a SDF and DDF. Increasing the oxygen flow rate decreases the flame height of the HMDSO-methane-oxygen diffusion flame as turbulence accelerates the mixing of fuel and oxidant.

Polymer Chains are Mass-Fractals

$R_{RMS} = n^{1/2}\, l$	Mass ~ Size^2
3-d object	Mass ~ Size^3
2-d object	Mass ~ Size^2
1-d object	Mass ~ Size^1
d_f-object	Mass ~ Size^{df}

This leads to odd properties:

density $$\rho = \frac{Mass}{Volume} = \frac{Mass}{Size^3} = \frac{Size^{d_f}}{Size^3} \sim Size^{d_f - 3}$$

For a 3-d object density doesn't depend on size,
For a 2-d object density drops with Size
Larger polymers are less dense

Mass Fractal dimension, d_f

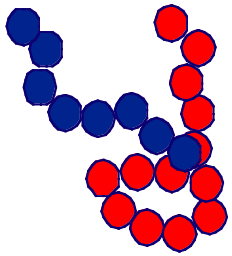

$$mass = z \sim \left(\frac{R}{d_p} \right)^{d_f}$$

z is mass/DOA
d_p is bead size
R is coil size

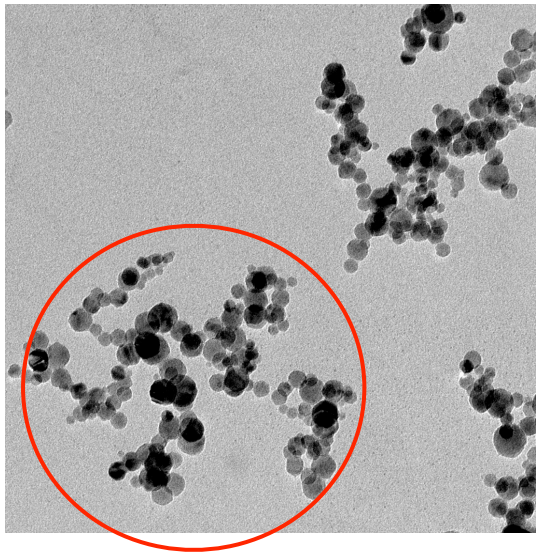

Nano-titania from Spray Flame

$R/d_p = 10$, $z \sim 220$
$d_f = \ln(220)/\ln(10) = 2.3$

Random Aggregation (right) $d_f \sim 1.8$
Randomly Branched Gaussian $d_f \sim 2.3$
Self-Avoiding Walk $d_f = 5/3$

Problem:
Disk $d_f = 2$
Gaussian Walk $d_f = 2$

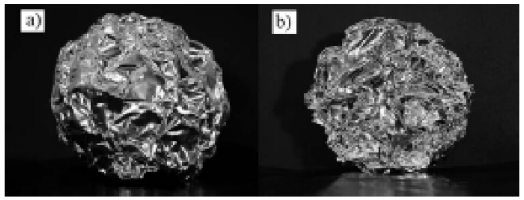

FIG. 1. Images of (a) balls folded from an aluminum sheet of thickness h=0.06 mm and edge size L=60 cm and (b) the cut through this ball. Balankin et al. (*Phys. Rev. E* **75** 051117

Mass Fractal dimension, d_f

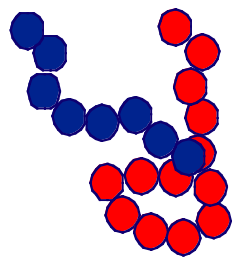

$$mass = z \sim \left(\frac{R}{d_p} \right)^{d_f}$$

z is mass/DOA
d_p is bead size
R is coil size

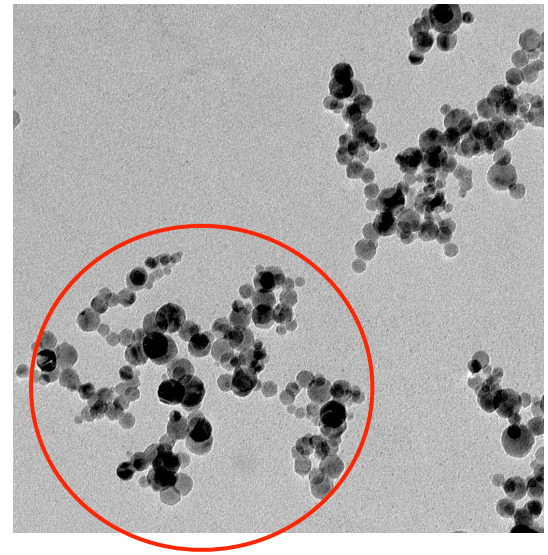

Nano-titania from Spray Flame

$R/d_p = 10$, $z \sim 220$
$d_f = \ln(220)/\ln(10) = 2.3$

Random Aggregation (right) $d_f \sim 1.8$
Randomly Branched Gaussian $d_f \sim 2.3$
Self-Avoiding Walk $d_f = 5/3$

Problem:
Disk $d_f = 2$
Gaussian Walk $d_f = 2$

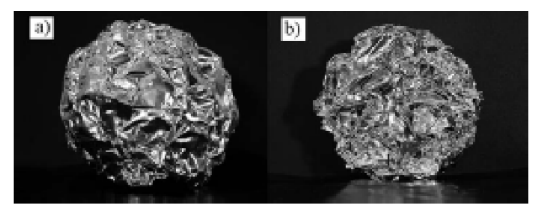

FIG. 1. Images of (a) balls folded from an aluminum sheet of thickness h=0.06 mm and edge size L=60 cm and (b) the cut through this ball. Balankin et al. (*Phys. Rev. E* **75** 051117

A measure of topology is not given by d_f.
Disk and coil are topologically different.
Foil and disk are topologically similar.

How Complex Mass Fractal Structures Can be Decomposed

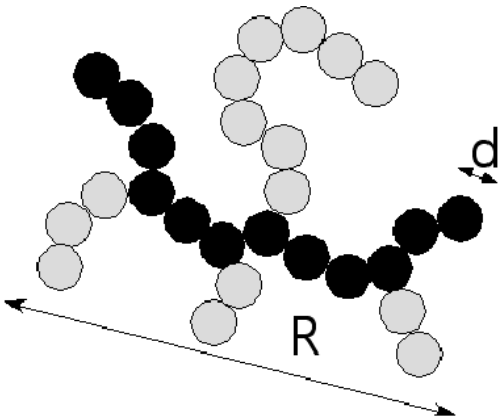

Tortuosity

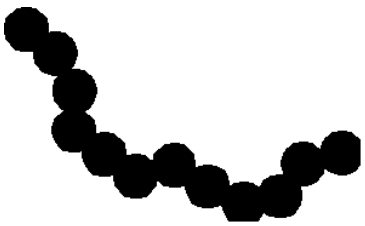

Connectivity

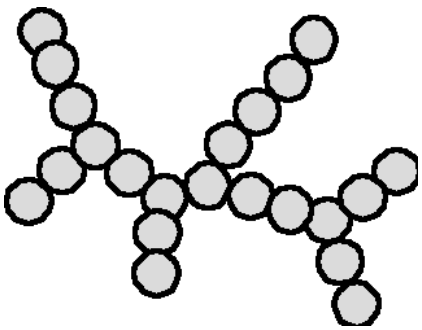

$$z \sim \left(\frac{R}{d}\right)^{d_f} \sim p^c \sim s^{d_{\min}}$$

$$p \sim \left(\frac{R}{d}\right)^{d_{\min}}$$

$$s \sim \left(\frac{R}{d}\right)^{c}$$

$$d_f = d_{\min} c$$

z	d_f	p	d_{min}	s	c	R/d
27	1.36	12	1.03	22	1.28	11.2

Consider a Crumpled Sheet

A 2-d Sheet has c = 2
d_{min} depends on the extent of crumpling

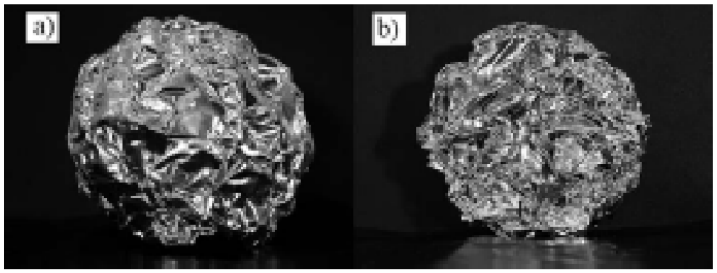

FIG. 1. Images of (a) balls folded from an aluminum sheet of thickness h=0.06 mm and edge size L=60 cm and (b) the cut through this ball.

$$d_f = 2.3$$
$$d_{\min} = 1.15$$
$$c = 2$$

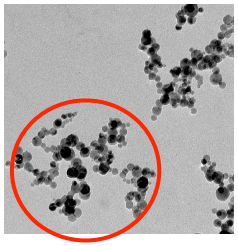

$$d_f = 2.3$$
$$d_{\min} = 1.47$$
$$c = 1.56$$

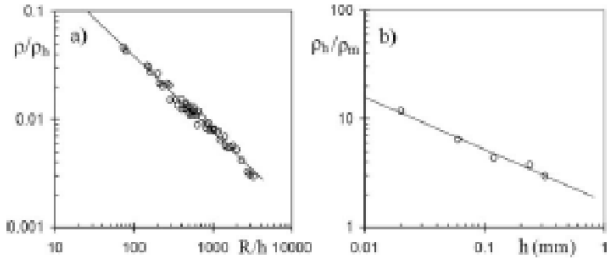

FIG. 3. (a) Data collapse for ρ/ρ_h versus R/h (the slope of the fitting line is $3-D=0.7009$, $R^2=0.98$); and (b) log-log plot of ρ_h/ρ_m versus h (straight line is given by $y=1.728x^{-0.4816}$, $R^2=0.98$).
Balankin et al. (*Phys. Rev. E* **75** 051117 (2007))

Disk

$$d_f = 2$$

$$d_{\min} = 1$$

$$c = 2$$

Extended β-sheet
(misfolded protein)

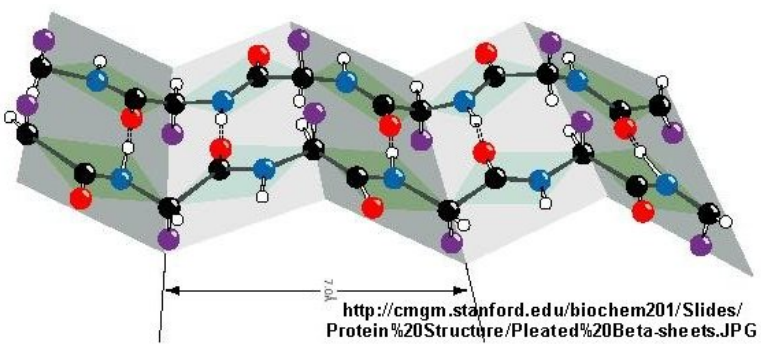

Random Coil

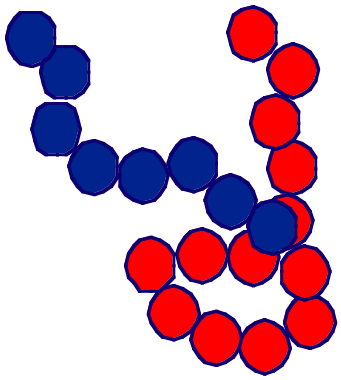

$$d_f = 2$$

$$d_{\min} = 2$$

$$c = 1$$

Unfolded Gaussian chain

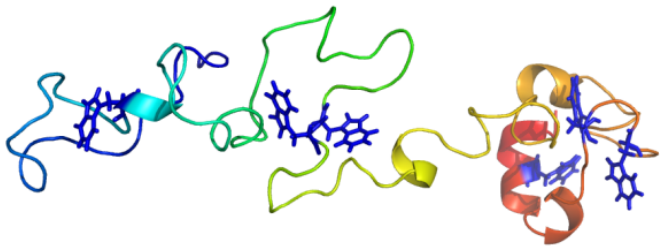

Primary Size for Fractal Aggregates

Primary Size for Fractal Aggregates

- Particle counting from TEM
- Gas adsorption V/S => d_p
- Static Scattering R_g, d_p
- Dynamic Light Scattering

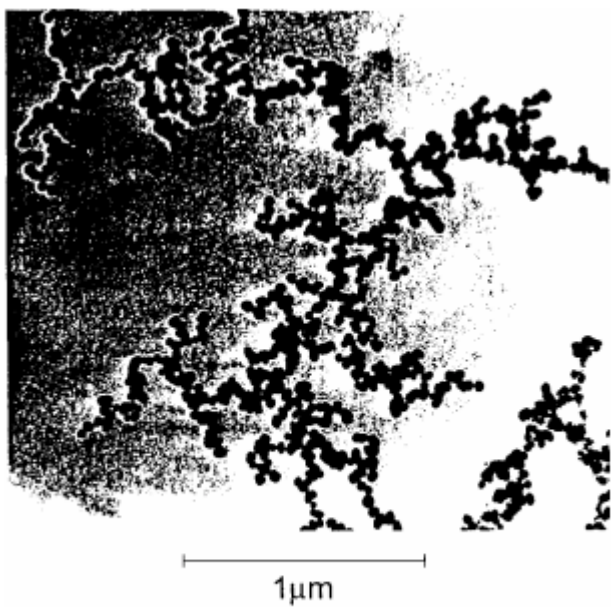

Figure 2. TEM picture of titania (TiO_2) fractal aggregates with $D \simeq 1.8$ produced by pyrolysis of Titanium Isopropoxide.

http://www.phys.ksu.edu/personal/sor/publications/2001/light.pdf

Cryo Scanning Electron Microscopy

A scanning electron micrograph of a frozen sample was taken. The sizes of the particles visible on the picture were measured individually with a ruler and used to calculate a number-mean, D(1,0), a volume-mean, D(4,3) and a number-distribution.

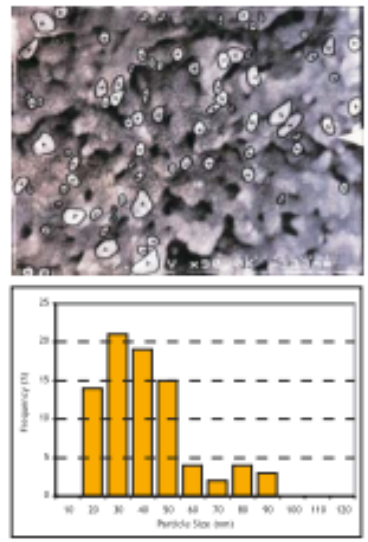

Number Mean - D(1,0) = 45.2 nm
Volume Mean - D(4,3) = 68.0 nm

Note : due to the limited number (82) of particles measured this result is only indicative.

http://www.koboproductsinc.com/Downloads/PS-Measurement-Poster-V40.pdf

Primary Size for Fractal Aggregates

- Particle counting from TEM
- Gas adsorption V/S => d_p
- Static Scattering R_g, d_p
- Dynamic Light Scattering

Dynamic Light Scattering

To evaluate repeatability and robustness, the measure was made 8 times, using 3 different dilutions. The following graph presents one of these measures, expressed as intensity-distribution, volume-distribution and number (length)-distribution.

Measure on Micomp Model 370 - samples diluted in chloroform to 200-350 kHz.

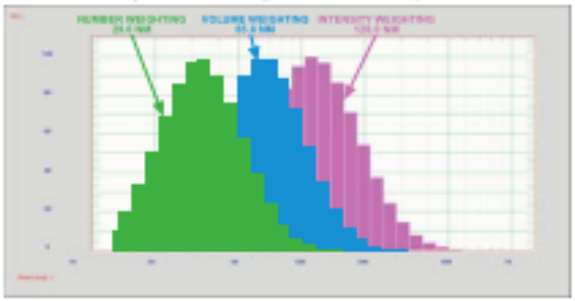

The following table shows the averaged results for the 8 measurements. Precision is calculated as the Relative Standard Deviation of the measurements.

Mean Calculation	Particle Size	Precision
Intensity Weighting	127.9 nm	2 %
Volume Weighting	71.6 nm	16 %
Number Weighting	36.2 nm	25 %

http://www.koboproductsinc.com/Downloads/PS-Measurement-Poster-V40.pdf

For static scattering p(r) is the binary spatial auto-correlation function

We can also consider correlations in time, binary temporal correlation function
$g_I(q,\tau)$

For dynamics we consider a single value of q or r and watch how the intensity changes with time
$I(q,t)$

We consider correlation between intensities separated by t
We need to subtract the constant intensity due to scattering at different size scales
and consider only the fluctuations at a given size scale, r or $2\pi/r = q$

Dynamic Light Scattering

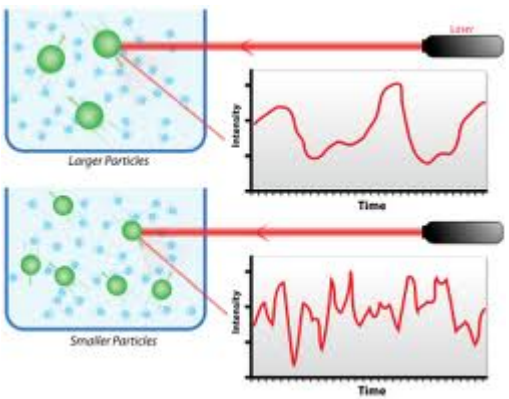

$$g^2(q;\tau) = \frac{\langle I(t)I(t+\tau)\rangle}{\langle I(t)\rangle^2}$$

$$g^2(q;\tau) = 1 + \beta\left[g^1(q;\tau)\right]^2$$

$$q = \frac{4\pi n_0}{\lambda}\sin\left(\frac{\theta}{2}\right)$$

$$g^1(q;\tau) = \exp(-\Gamma\tau)$$

$$\Gamma = q^2 D_t$$

$$D = k_B T / 6\pi\eta a$$

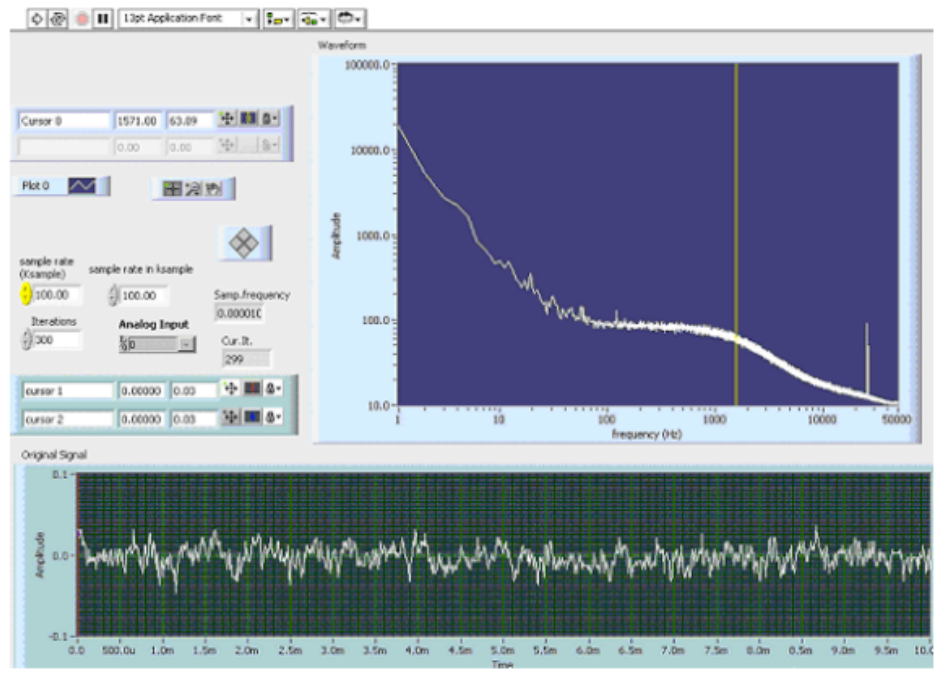

a = R_H = Hydrodynamic Radius

Dynamic Light Scattering

my DLS web page

http://www.eng.uc.edu/~gbeaucag/Classes/Physics/DLS.pdf

Wiki

http://webcache.googleusercontent.com/search?q=cache:eY3xhiX117IJ:en.wikipedia.org/wiki/Dynamic_light_scattering+&cd=1&hl=en&ct=clnk&gl=us

Wiki Einstein Stokes

http://webcache.googleusercontent.com/search?q=cache:yZDPRbqZ1BIJ:en.wikipedia.org/wiki/Einstein_relation_(kinetic_theory)+&cd=1&hl=en&ct=clnk&gl=us

Gas Adsorption

$$\theta = \frac{\text{adsorbed sites}}{\text{total sites (N)}}$$

A + S <=> AS

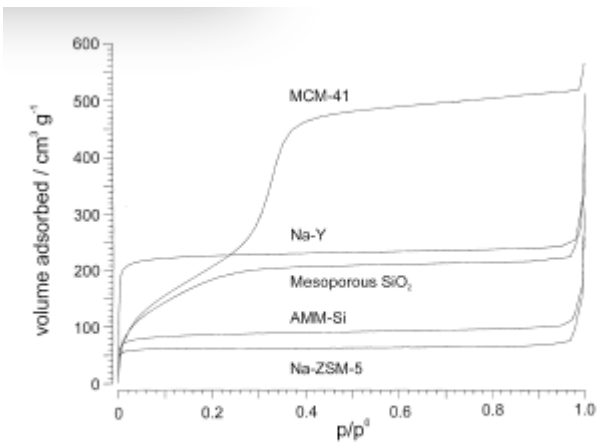

Fig. 2. Adsorption isotherms of the samples tested with Ar at 87.5 K.

Adsorption

$$\frac{d\theta}{dt} = k_a p N (1-\theta)$$

Equilibrium

=

Desorption

$$\frac{d\theta}{dt} = k_d N \theta$$

$$\theta = \frac{Kp}{1+Kp}$$

$$K = k_a / k_d$$

$$\frac{\partial \ln K}{\partial T} = \frac{\Delta H_{abs}}{RT^2}$$

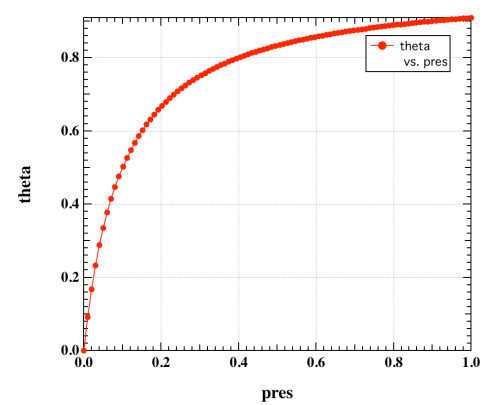

http://www.chem.ufl.edu/~itl/4411L_f00/ads/ads_1.html

Gas Adsorption

Multilayer adsorption

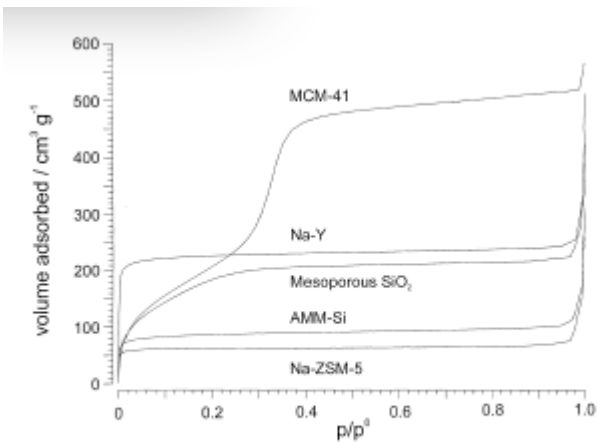

Fig. 2. Adsorption isotherms of the samples tested with Ar at 87.5 K.

BET Isotherm

Various Values of c

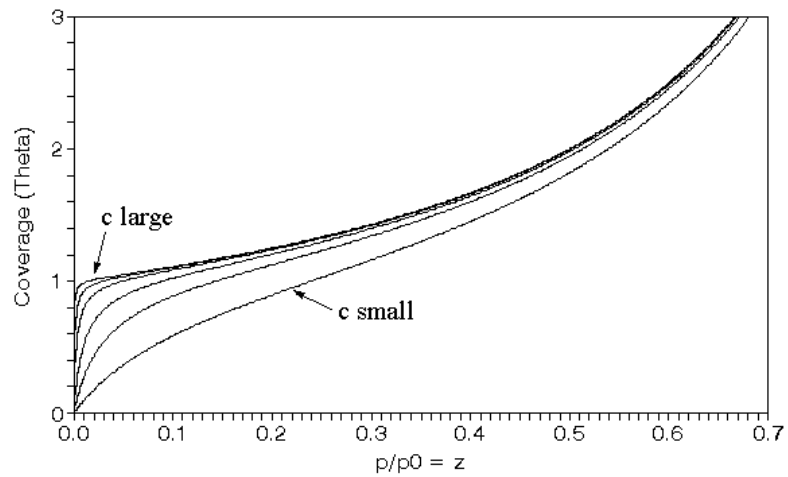

$$\frac{n}{n_{mono}} = \frac{cz}{(1-z)\,[1 - z(1-c)]} = (\theta)$$

$$c \approx \frac{e^{-\Delta H_{ads}/RT}}{e^{\Delta H_{vap}/RT}}$$

http://www.chem.ufl.edu/~itl/4411L_f00/ads/ads_1.html

S. Storck et al. / Applied Catalysis A: General 174 (1998) 137–146

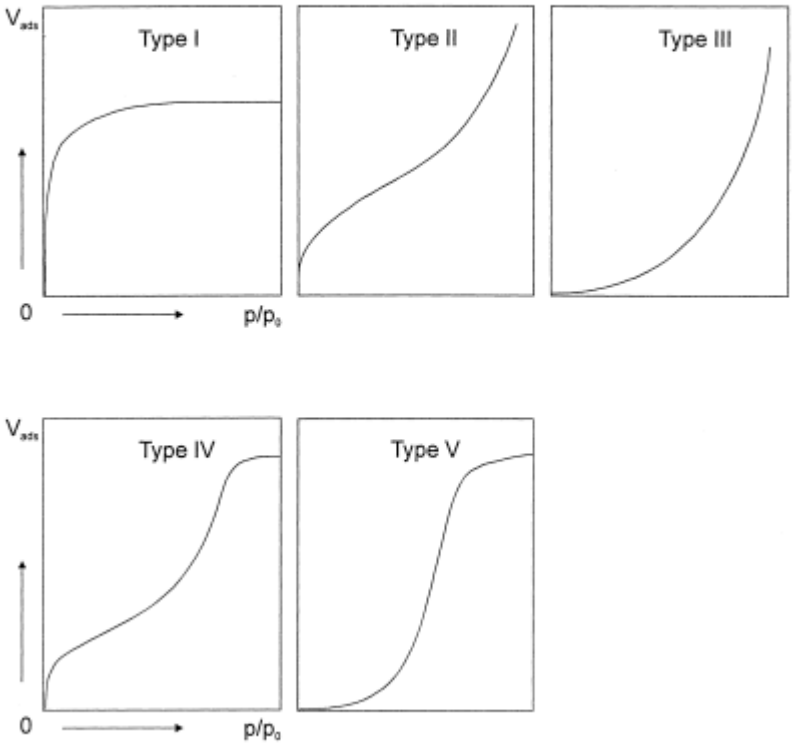

Fig. 1. Adsorption isotherm types defined by Brunauer [6].

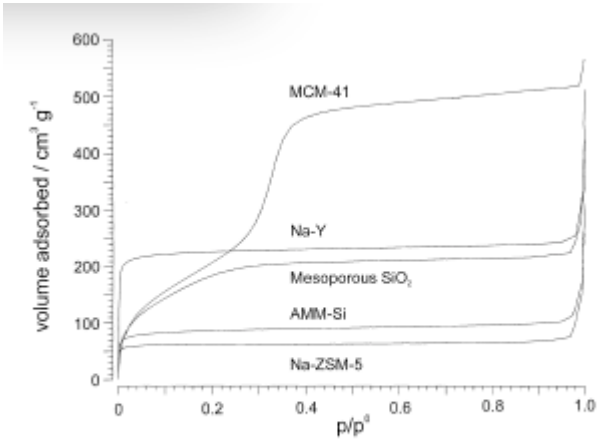

Fig. 2. Adsorption isotherms of the samples tested with Ar at 87.5 K.

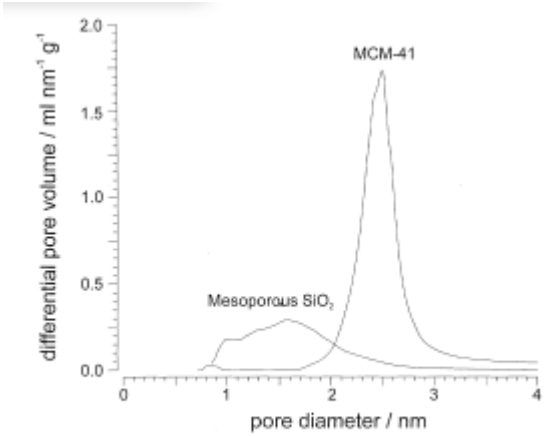

Fig. 3. Pore-size distribution according to the BJH method.

http://www.eng.uc.edu/~gbeaucag/Classes/Nanopowders/GasAdsorptionReviews/ReviewofGasAdsorptionGOodOne.pdf

From gas adsorption obtain surface area by number of gas atoms times an area for the adsorbed gas atoms in a monolayer

Have a volume from the mass and density.

So you have S/V or V/S

Assume sphere $S = 4\pi R^2$, $V = 4/3\ \pi R^3$

So $d_p = 6V/S$

Sauter Mean Diameter $d_p = \langle R^3 \rangle / \langle R^2 \rangle$

Log-Normal Distribution

$$f(R) = \frac{1}{R\sigma(2\pi)^{1/2}} \exp\left\{ -\frac{[\log(R/m)]^2}{2\sigma^2} \right\},$$

$$\langle R^r \rangle = m^r \exp\left(r^2\sigma^2/2\right) = \exp\left(r\mu + r^2\sigma^2/2\right)$$

$$\langle R \rangle = m \exp\left(\sigma^2/2\right)$$

Mean

$$\sigma_g = \exp(\sigma) \quad \mathrm{x}_g = \exp(m)$$

Geometric standard deviation and geometric mean (median)

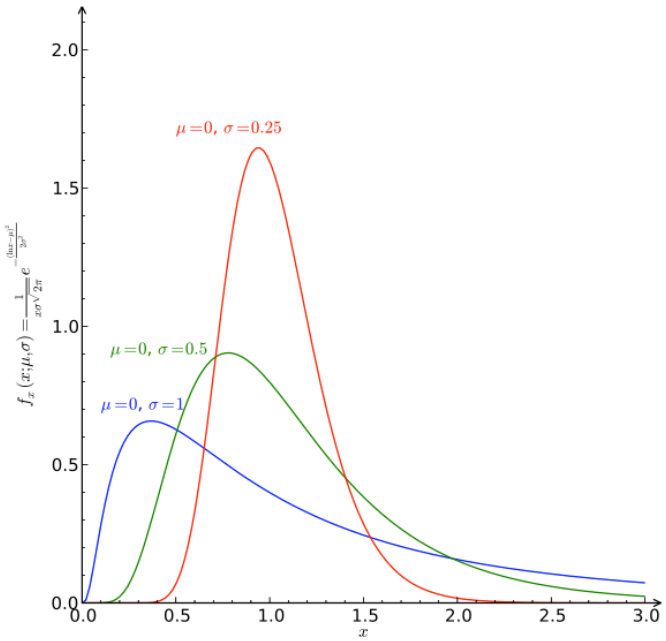

Gaussian is centered at the Mean and is symmetric. For values that are positive (size) we need an asymmetric distribution function that has only values for greater than 1. In random processes we have a minimum size with high probability and diminishing probability for larger values.

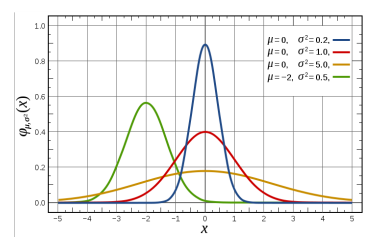

http://www.eng.uc.edu/~gbeaucag/PDFPapers/ks5024%20Japplcryst%20Beaucage%20PSD.pdf

http://en.wikipedia.org/wiki/Log-normal_distribution

Log-Normal Distribution

$$f(R) = \frac{1}{R\sigma(2\pi)^{1/2}} \exp\left\{ -\frac{[\log(R/m)]^2}{2\sigma^2} \right\},$$

$$\langle R^r \rangle = m^r \exp\left(r^2\sigma^2/2\right) = \exp\left(r\mu + r^2\sigma^2/2\right)$$

$$\langle R \rangle = m \exp\left(\sigma^2/2\right)$$

Mean

$$\sigma_g = \exp(\sigma) \quad x_g = \exp(m)$$

Geometric standard deviation and geometric mean (median)

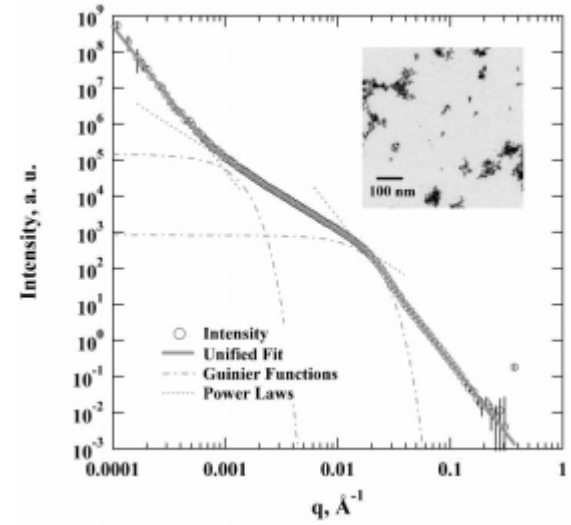

Static Scattering Determination of Log Normal Parameters

$$\ln \sigma_g = \sigma = \left\{ \frac{\ln\left[B\left(R_g^2\right)^2/(1.62G)\right]}{12} \right\}^{1/2} = \left(\frac{\ln \mathrm{PDI}}{12}\right)^{1/2} \quad (17)$$

and

$$m = \left\{5R_g^2/[3\exp(14\sigma^2)]\right\}^{1/2}, \quad (18)$$

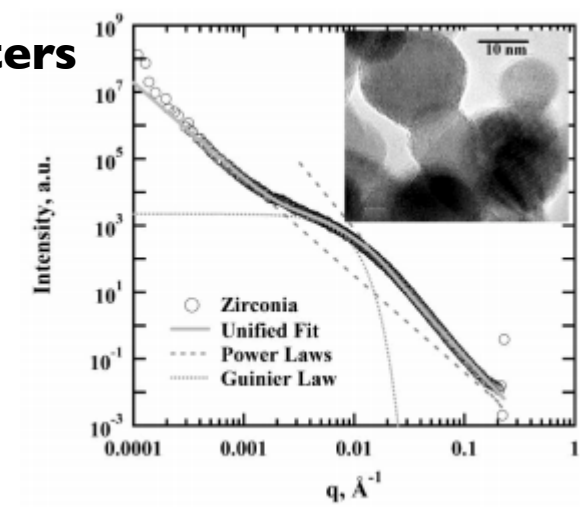

http://www.eng.uc.edu/~gbeaucag/PDFPapers/ks5024%20Japplcryst%20Beaucage%20PSD.pdf

Primary Size for Fractal Aggregates

- Particle counting from TEM
- Gas adsorption V/S => d_p
- Static Scattering R_g, d_p
- Dynamic Light Scattering

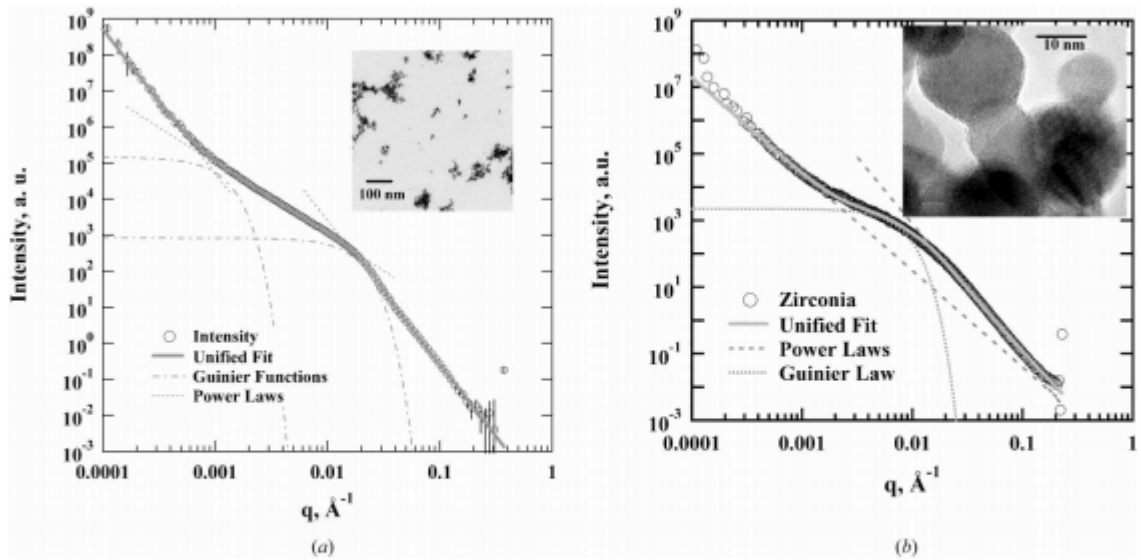

Figure 2
USAXS data from aggregated nanoparticles (circles) showing unified fits (bold grey lines), primary particle Guinier and Porod functions at high q, the intermediate mass fractal scaling regime and the aggregate Guinier regime (dashed lines). (*a*) Fumed titania sample with multi-grain particles and low-q excess scattering due to soft agglomerates. $d_{V/S}$ = 16.7 nm (corrected to 18.0 nm), PDI = 3.01 (σ_g = 1.35), R_g = 11.2 nm, d_f = 1.99, $z_{\Sigma 1}$ = 175, z_{R_g} = 226, R_{g2} = 171 nm. From gas adsorption, d_p = 16.2 nm. (*b*) Fumed zirconia sample (Mueller *et al.*, 2004) with single-grain particles, as shown in the inset. The primary particles for this sample have high polydispersity leading to the observed hump near the primary particle scattering regime. $d_{V/S}$ = 20.3 nm, PDI = 10.8 (σ_g = 1.56), R_g = 26.5 nm, d_f = 2.90. From gas adsorption, d_p = 19.7 nm.

http://www.eng.uc.edu/~gbeaucag/PDFPapers/ks5024%20Japplcryst%20Beaucage%20PSD.pdf

Primary Size for Fractal Aggregates

- **Particle counting from TEM**
- **Gas adsorption V/S => d_p**
- **Static Scattering R_g, d_p**

Smaller Size = Higher S/V
(Closed Pores or similar issues)

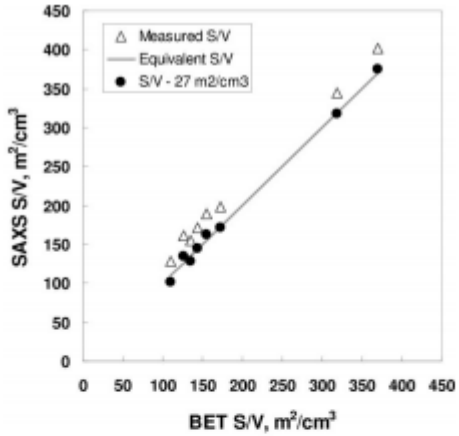

(a)

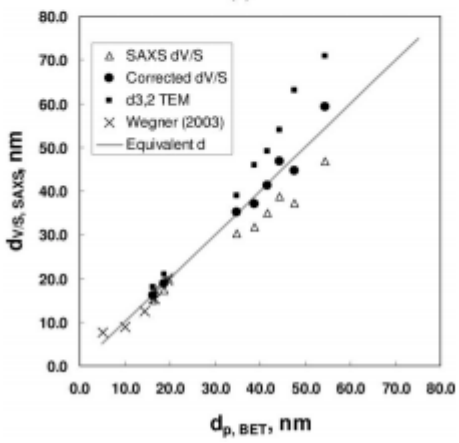

(b)

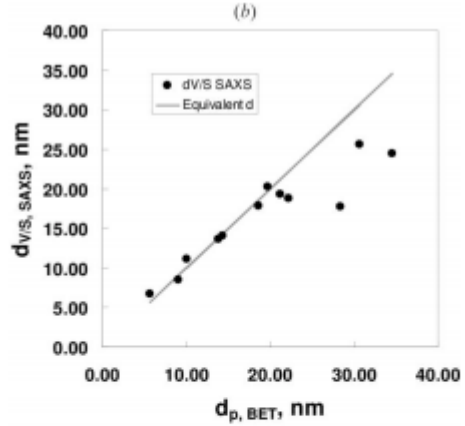

(c)

Figure 3
(*a*) *S/V* from SAXS for titania particles produced by vapor-phase pyrolysis of titania tetraisopropoxide by Kammler *et al.* (2002, 2003). The SAXS *S/V* can be made to agree with the BET value by subtraction of 27 $m^2\ cm^{-3}$. (*b*) $d_{V/S}$ from USAXS [and corrected from (*a*)] *versus* d_p from BET analysis of gas adsorption data for a series of titania samples produced by Kammler (triangles and filled circles), and samples made in a quenched-spray flame from Wegner & Pratsinis (2003) (crosses, single-grain particles). The calculated $d_{3,2}$ from TEM micrographs for the Kammler samples is also shown (filled squares). (*c*) $d_{V/S}$ from USAXS *versus* d_p from BET for fumed zirconia samples of Mueller *et al.* (2004).

http://www.eng.uc.edu/~gbeaucag/PDFPapers/ks5024%20Japplcryst%20Beaucage%20PSD.pdf

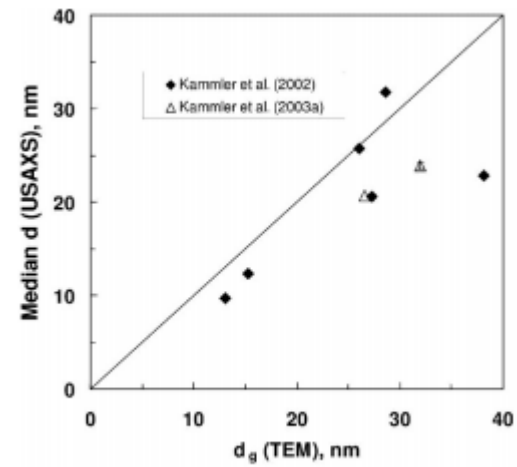

(a)

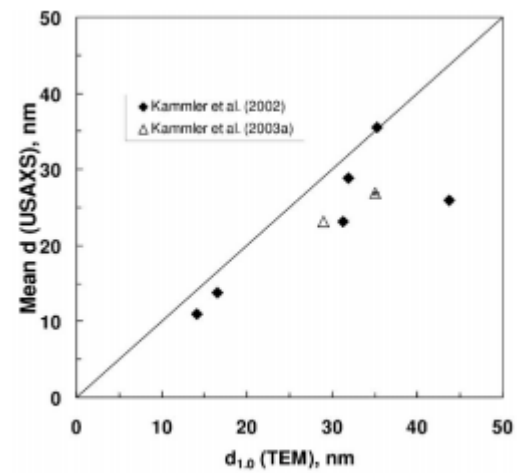

(b)

(a) (b)

Figure 4
(*a*) Comparison of the median particle size from exp *m*, with *m* defined by equation (18), and the median particle size calculated from an analysis of TEM data on TiO_2. (*b*) Mean particle size, ⟨*R*⟩ from USAXS, equation (2) with *r* = 1, and from TEM (Kammler *et al.*, 2003) for the same samples as Figs. 3(*a*) and 3(*b*).

Fractal Aggregates and Agglomerates

Primary Size for Fractal Aggregates

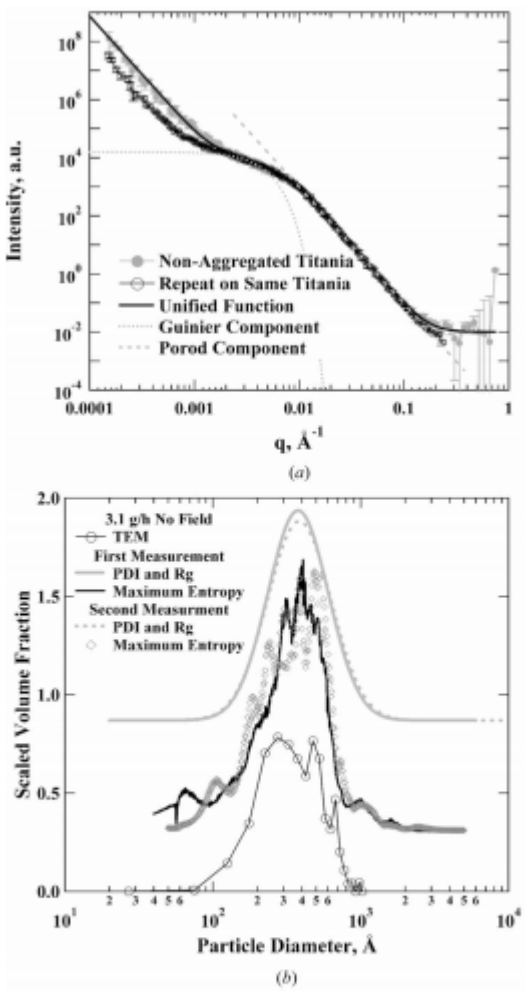

Figure 5
3.1 g h^{-1} titania. (*a*) Repeat USAXS runs on a non-aggregated titania powder (Fig. 1). (*b*) Particle size distributions from TEM (circles; Kammler *et al.*, 2003), equations (1), (2), (17) and (18) using PDI and R_g, and using the maximum-entropy program of Jemian (Jemian *et al.*, 1991). Distribution curves are shifted vertically for clarity. d_{VS} = 34.9 nm, PDI = 14.4 (σ_g = 1.60), R_g = 44.2 nm.

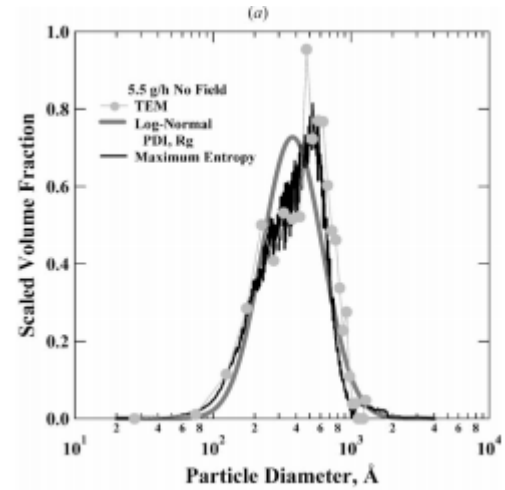

Fractal Aggregate Primary Particles

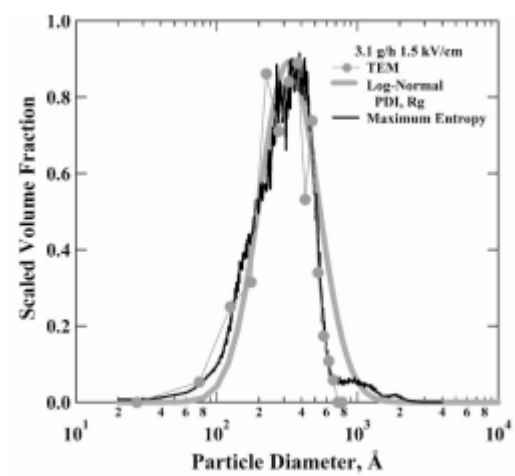

http://www.eng.uc.edu/~gbeaucag/PDFPapers/ks5024%20Japplcryst%20Beaucage%20PSD.pdf

Fractal Aggregates and Agglomerates
Aggregate growth

Some Issues to Consider for Aggregation/Agglomeration

Path of Approach, Diffusive or Ballistic (Persistence of velocity for particles)
Concentration of Monomers
persistence length of velocity compared to mean separation distance
Branching and structural complexity

What happens when monomers or clusters get to a growth site:
Diffusion Limited Aggregation
Reaction Limited Aggregation

Chain Growth (Monomer-Cluster), Step Growth (Monomer-Monomer to Cluster-Cluster)
or a Combination of Both (mass versus time plots)

Cluster-Cluster Aggregation
Monomer-Cluster Aggregation
Monomer-Monomer Aggregation

DLCA Diffusion Limited Cluster-Cluster Aggregation
RLCA Reaction Limited Cluster Aggregation

Post Growth: Internal Rearrangement/Sintering/Coalescence/Ostwald Ripening

http://www.eng.uc.edu/~gbeaucag/Classes/Nanopowders/AggregateGrowth.pdf

Fractal Aggregates and Agglomerates

Aggregate growth

Consider what might effect the dimension of a growing aggregate.

Transport Diffusion/Ballistic
Growth Early/Late (0-d point => Linear 1-d => Convoluted 2-d => Branched 2+d)
Speed of Transport Cluster, Monomer
Shielding of Interior
Rearrangement
Sintering
Primary Particle Shape

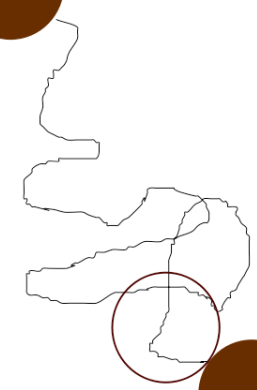

DLA df = 2.5 Monomer-Cluster (Meakin 1980 Low Concentration)
DLCA df = 1.8 (Higher Concentration Meakin 1985)

Ballistic Monomer-Cluster (low concentration) df = 3
Ballistic Cluster-Cluster (high concentration) df = 1.95

Fractal Aggregates and Agglomerates

Aggregate growth

Colloids with Strongly attractive forces

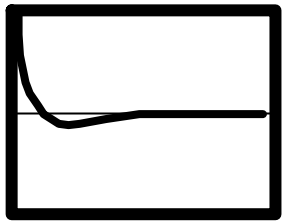

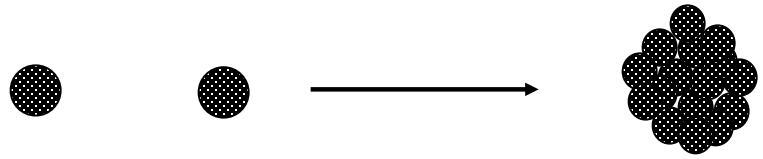

NEAR EQUILIBRIUM: Ostwald Ripening

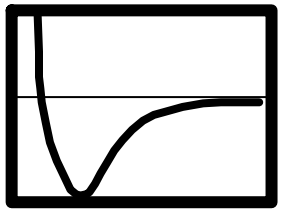

Kinetic Growth: DIFFUSION LIMITED

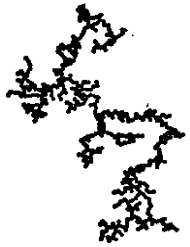

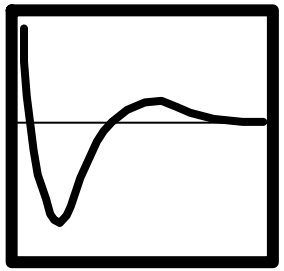

Kinetic Growth: CHEMICALLY LIMITED

Reaction Limited,
Short persistence of velocity

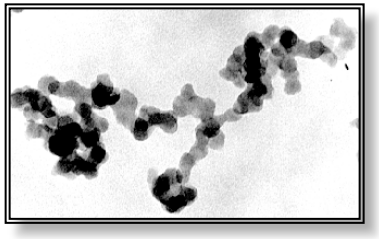

Precipitated Silica

From DW Schaefer Class Notes

Fractal Aggregates and Agglomerates

Aggregate growth

Sticking Law

Particle-Cluster Growth

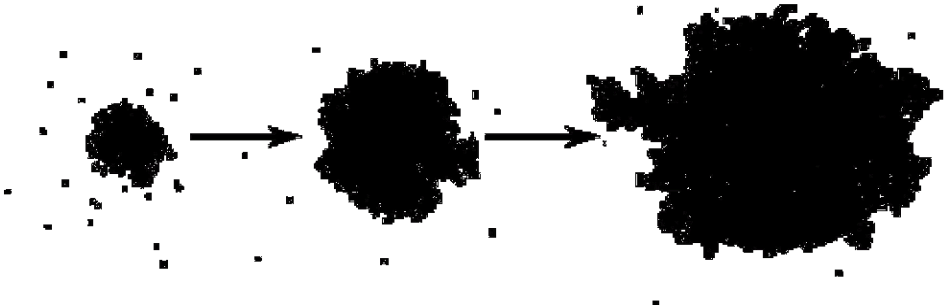

Cluster-Cluster Growth

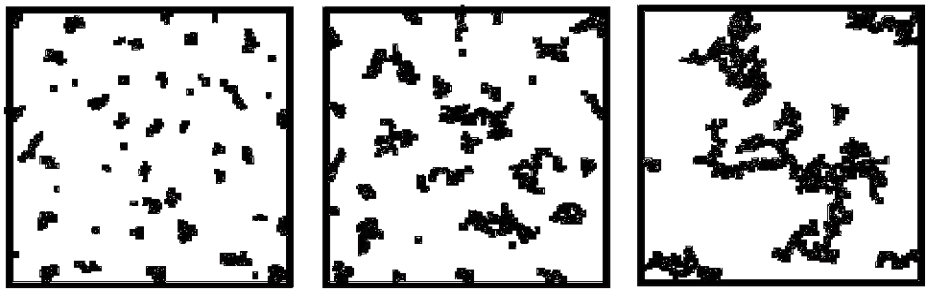

From DW Schaefer Class Notes

Fractal Aggregates and Agglomerates

Aggregate growth

Transport

Diffusion-Limited

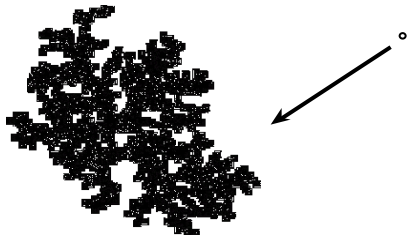

Ballistic

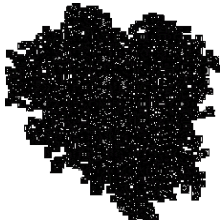

Reaction-Limited
(Independent of transport)

From DW Schaefer Class Notes

Fractal Aggregates and Agglomerates

Aggregate growth

Aggregation Models

Eden Model particles are added at random with equal probability to any unoccupied site adjacent to one or more occupied sites
(Surface Fractals are Produced)

Vold-Sutherland Model particles with random **linear** trajectories are added to a growing cluster of particles at the position where they first contact the cluster

Witten-Sander Model particles with random **Brownian** trajectories are added to a growing cluster of particles at the position where they first contact the cluster

Transport

Sticking Law	Reaction-Limited	Ballistic	Diffusion-Limited
Monomer-Cluster	EDEN 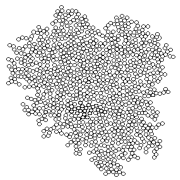 D = 3.00	VOLD 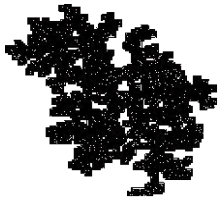 D = 3.00	WITTEN-SANDER 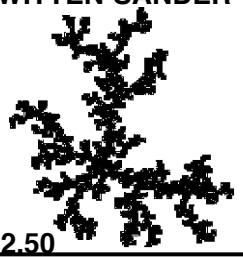 D = 2.50
Cluster-Cluster	RLCA  D = 2.09	SUTHERLAND  D = 1.95	DLCA 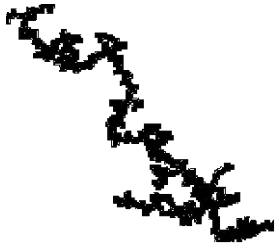 D = 1.80

In RLCA a "sticking probability is introduced in the random growth process of clusters. This increases the dimension.

Sutherland Model pairs of particles are assembled into randomly oriented dimers. Dimers are coupled at random to construct tetramers, then octoamers etc. This is a step-growth process except that all reactions occur synchronously (monodisperse system).

In DLCA the "sticking probability is 1. Clusters follow random walk.

From DW Schaefer Class Notes

2 PAUL MEAKIN

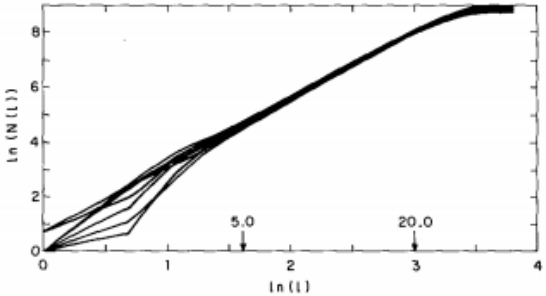

FIG. 8. Dependence of ln ($N(l)$) on ln (l) for eight clusters grown using the WS model of diffusion-limited cluster formation on a three-dimensional cubic lattice.

http://www.eng.uc.edu/~gbeaucag/Classes/MorphologyofComplexMaterials/MeakinVoldSunderlandEdenWittenSanders.pdf

Fractal Aggregates and Agglomerates

Aggregate growth

Analysis of Fractals

$$\mathrm{Log}(N) = D\,\mathrm{Log}(R)$$

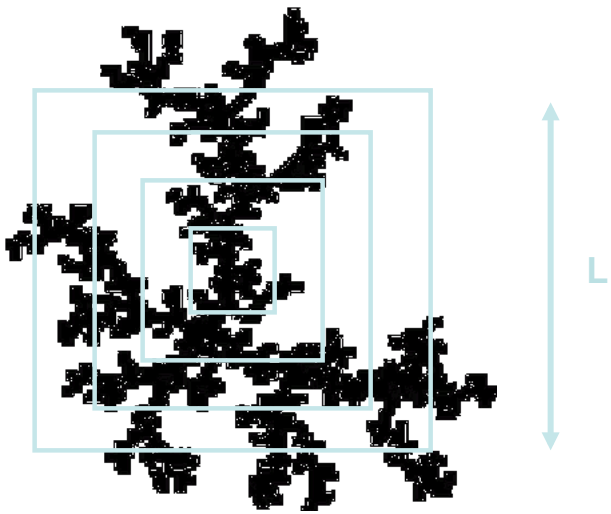

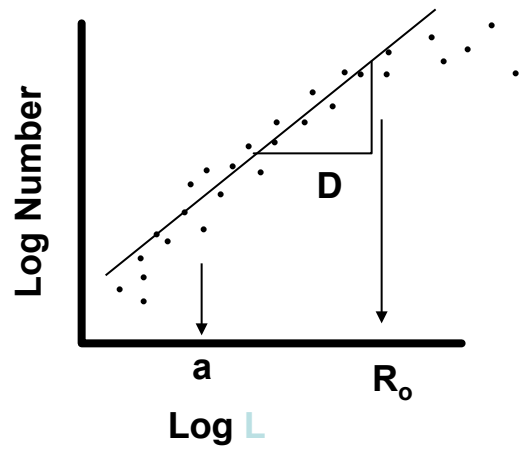

From DW Schaefer Class Notes

Fractal Aggregates and Agglomerates

Aggregate growth

Self Similarity

Euclidian Objects

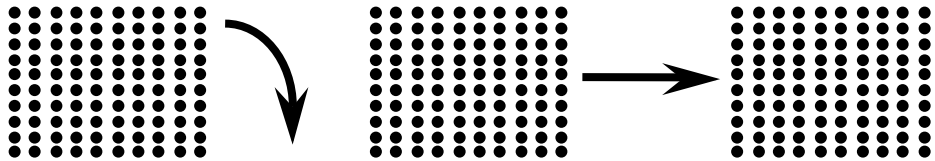

Fractal Objects

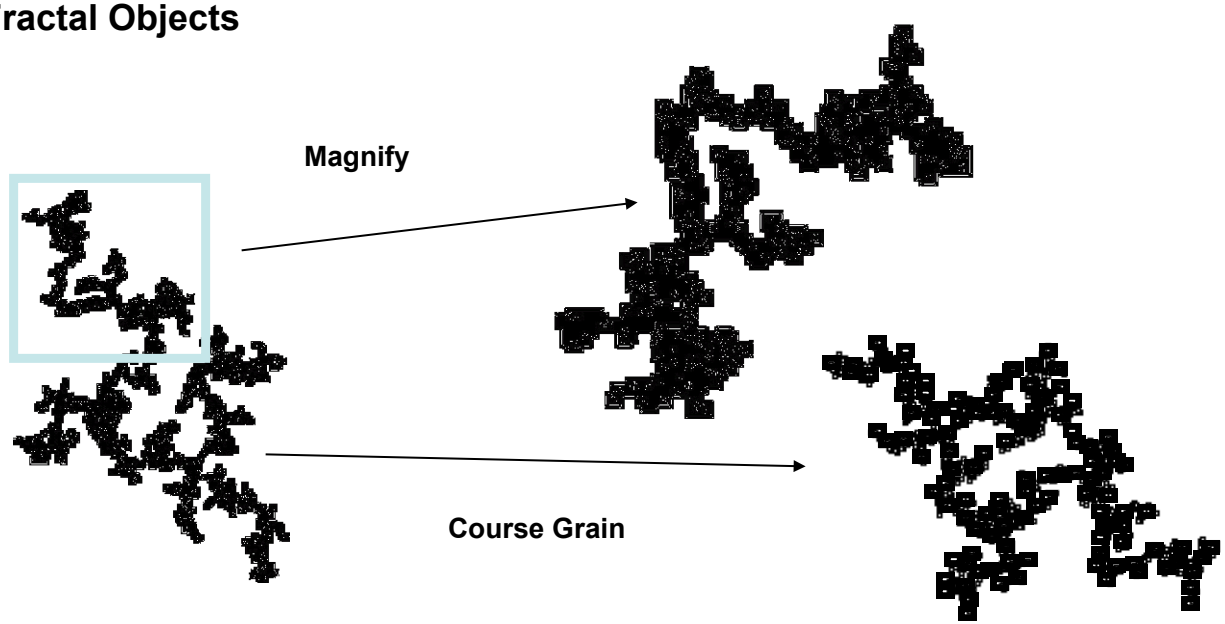

From DW Schaefer Class Notes

Fractal Aggregates and Agglomerates

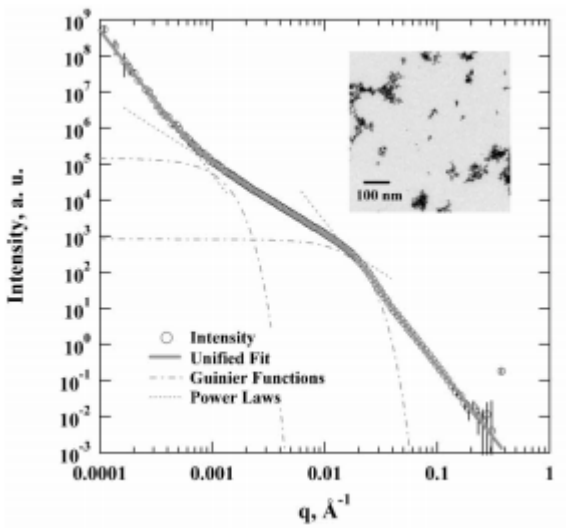

Primary: Primary Particles
Secondary: Aggregates
Tertiary: Agglomerates

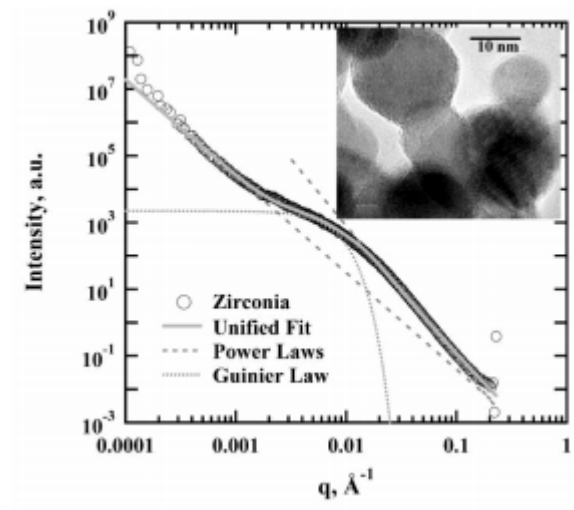

Primary: Primary Particles

Tertiary: Agglomerates

From DW Schaefer Class Notes

http://www.eng.uc.edu/~gbeaucag/PDFPapers/ks5024%20Japplcryst%20Beaucage%20PSD.pdf

Hierarchy of Polymer Chain Dynamics

Dilute Solution Chain

Dynamics of the chain

Harmonic Oscillator

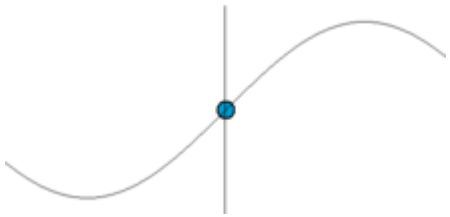

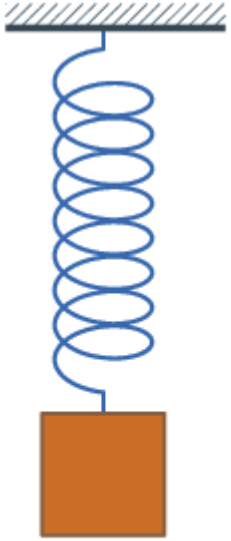

Damped Harmonic Oscillator

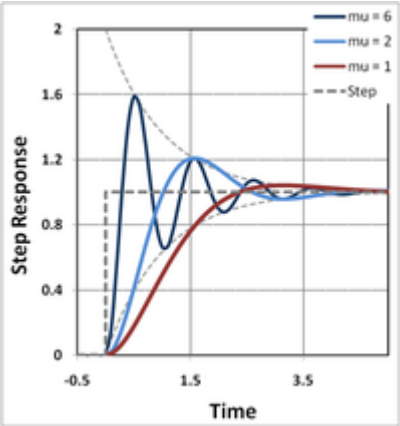

Dilute Solution Chain

Dynamics of the chain

Damped Harmonic Oscillator

$$E(x) = \frac{k_{spr} x^2}{2}$$

$$\frac{dx}{dt} = \frac{-(dE/dx)}{\xi}$$

$$\xi = 6\pi\eta_{solvent} a$$

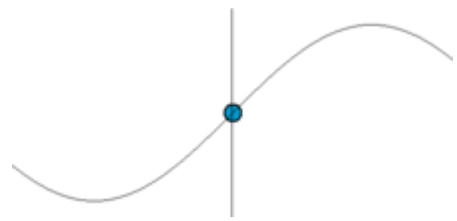

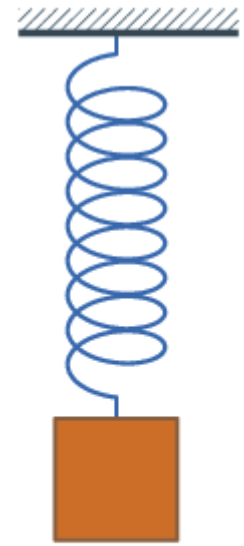

g(t) = random thermal motion

$$\frac{dx}{dt} = \frac{-k_{spr} x}{\xi} + g(t)$$

$$x(t) = \int_{-\infty}^{t} dt' \exp\left(-k_{spr}(t-t')/\xi\right) g(t')$$

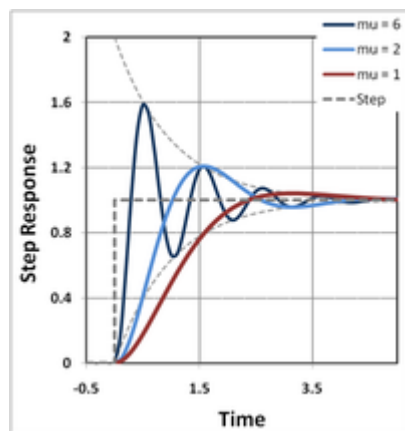

The exponential term is the "response function"
response to a pulse perturbation

Dilute Solution Chain

Dynamics of the chain

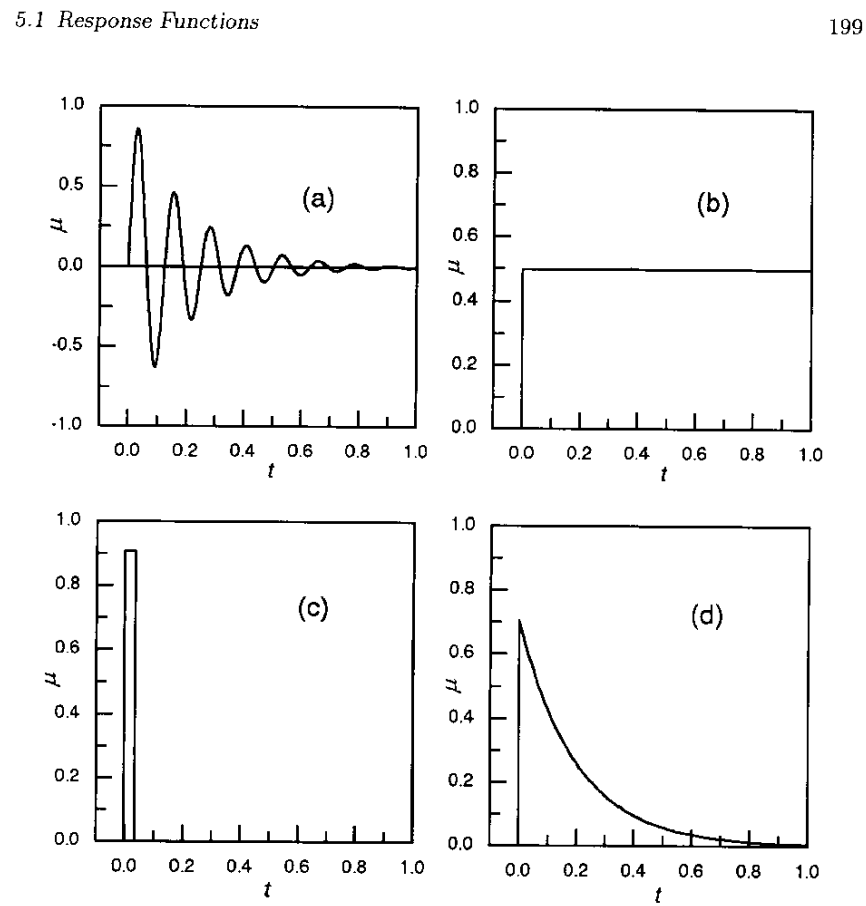

Fig. 5.4. Primary response function of a damped harmonic oscillator (a), a perfectly viscous body (b), a Hookean solid (c), a simple relaxatory system (d)

$$x(t) = \int_{-\infty}^{t} dt' \exp\left(-k_{spr}\left(t-t'\right)/\xi\right) g\left(t'\right)$$

The exponential term is the "response function"

response to a pulse perturbation

Dilute Solution Chain

Dynamics of the chain

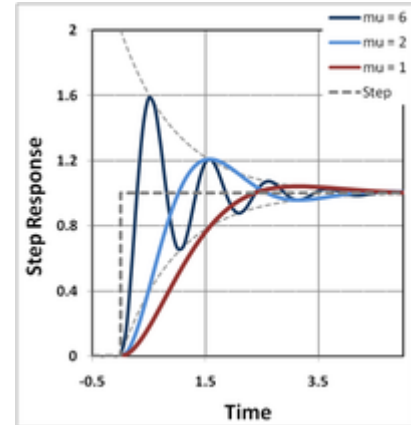

Damped Harmonic Oscillator

$$x(t) = \int_{-\infty}^{t} dt' \exp\left(-k_{spr}(t-t')/\xi\right) g(t')$$

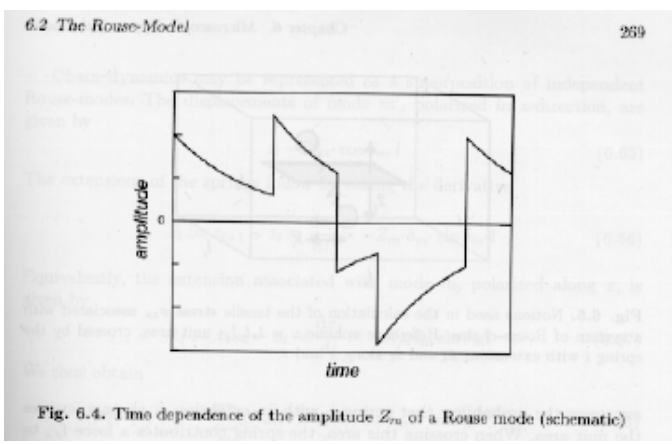

Fig. 6.4. Time dependence of the amplitude Z_{ru} of a Rouse mode (schematic)

For Brownian motion
of a harmonic bead in a solvent
this response function can be used to calculate the
time correlation function <x(t)x(0)>
for DLS for instance

$$\langle x(t)x(0)\rangle = \int_{-\infty}^{t} dt_1 \int_{-\infty}^{0} dt_2 \exp\left[-k_{spr}(t-t_1-t_2)/\xi\right]\langle g(t_1)g(t_2)\rangle$$

$$\langle g(t_1)g(t_2)\rangle = \frac{2kT}{\xi}\partial(t_1-t_2)$$

$$\langle x(t)x(0)\rangle = \frac{kT}{k_{spr}}\exp(-t/\tau)$$

τ is a relaxation time.

$$\tau = \frac{\xi}{k_{spr}}$$

Dilute Solution Chain

Dynamics of the chain

Rouse Motion

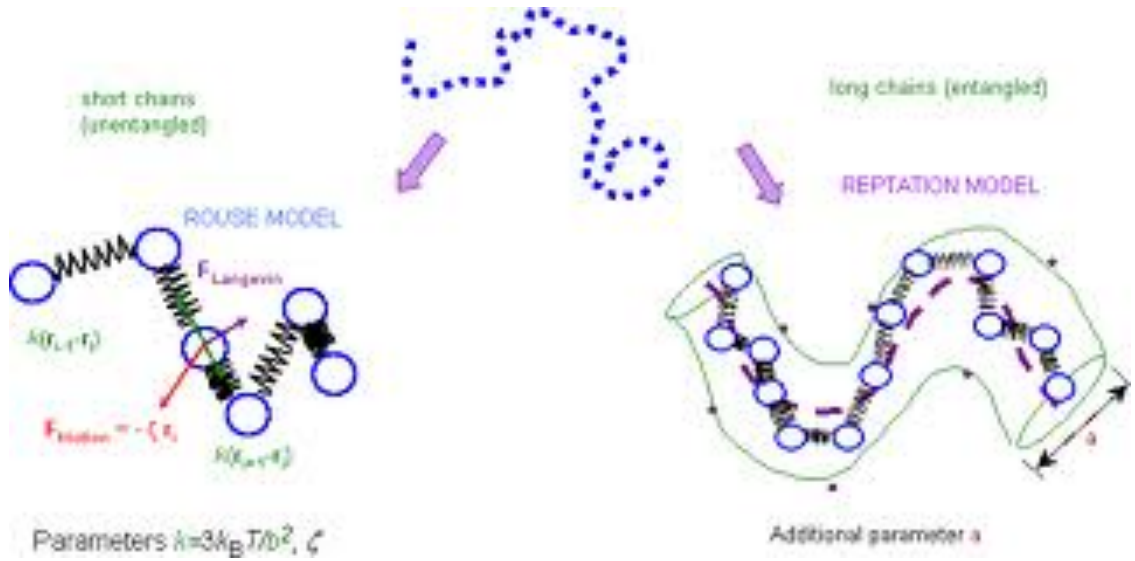

$$E = \frac{k_{spr}}{2}\sum_{i=1}^{N}\left(R_i - R_{i-1}\right)^2$$

$$\frac{dR_i}{dt} = \frac{-\left(dE/dR_i\right)}{\xi} + g_i(t)$$

$$\xi = 6\pi\eta_{solvent}a$$

Beads 0 and N are special

For Beads 1 to N-1

$$\frac{dR_i}{dt} = \frac{-k_{spr}}{\xi}\left(R_{i+1} + R_{i-1} - 2R_i\right) + g_i(t)$$

For Bead 0 use $R_{-1} = R_0$ and for bead N $R_{N+1} = R_N$

This is called a closure relationship

Dilute Solution Chain

Dynamics of the chain

Rouse Motion

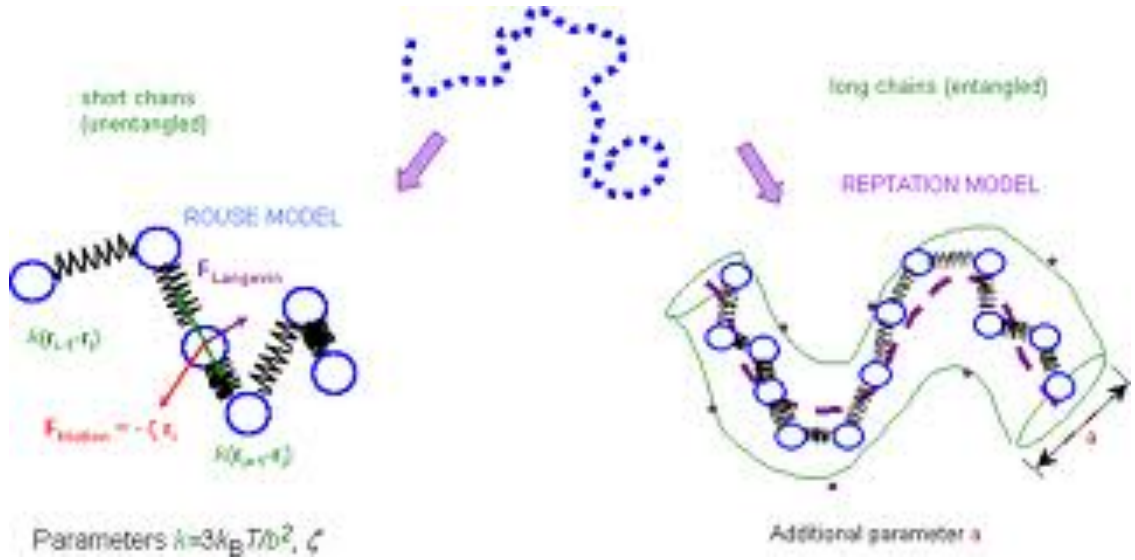

$$\frac{dR_i}{dt} = \frac{-k_{spr}}{\xi}\left(R_{i+1} + R_{i-1} - 2R_i\right) + g_i(t)$$

The Rouse unit size is arbitrary so we can make it very small and:

$$\frac{dR}{dt} = \frac{-k_{spr}}{\xi}\frac{d^2R}{di^2} + g_i(t)$$

With dR/dt = 0 at i = 0 and N

$$\frac{d^2R}{di^2}$$

Reflects the curvature of R in i,
it describes modes of vibration like on a guitar string

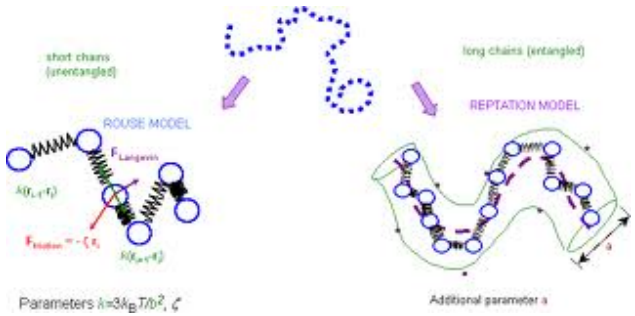

Dilute Solution Chain

Dynamics of the chain

Rouse Motion

$$\frac{d^2R}{di^2}$$ Describes modes of vibration like on a guitar string

For the "p'th" mode (0'th mode is the whole chain (string))

$$k_{spr,p} = \frac{2p^2\pi^2 k_{spr}}{N} = \frac{6\pi^2 kT}{Nb^2}p^2 \qquad \xi_p = 2N\xi \qquad \xi_0 = N\xi$$

$$\tau_p = \frac{\xi_p}{k_{spr,p}} = \frac{2N^2b^2\xi}{3\pi^2p^2kT}$$

Dilute Solution Chain

Dynamics of the chain

Rouse Motion

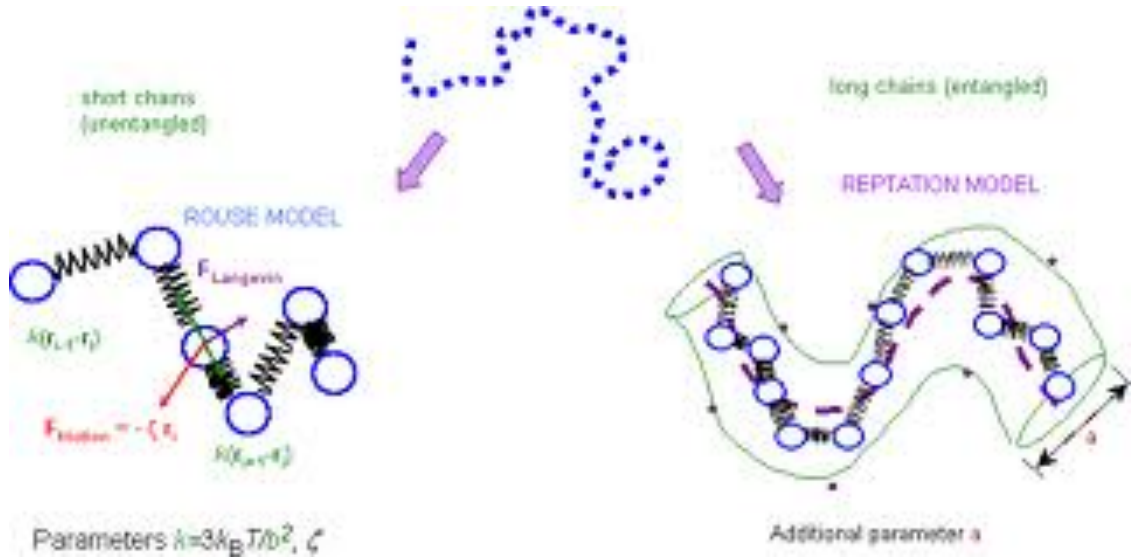

Predicts that the viscosity will follow N which is true for low molecular weights in the melt and for fully draining polymers in solution

Rouse model predicts
Relaxation time follows N^2 (actually follows N^3/df)
Diffusion constant follows 1/N (zeroth order mode is translation of the molecule) (actually follows $N^{-1/df}$)
Both failings are due to hydrodynamic interactions (incomplete draining of coil)

Dilute Solution Chain

Dynamics of the chain

Rouse Motion

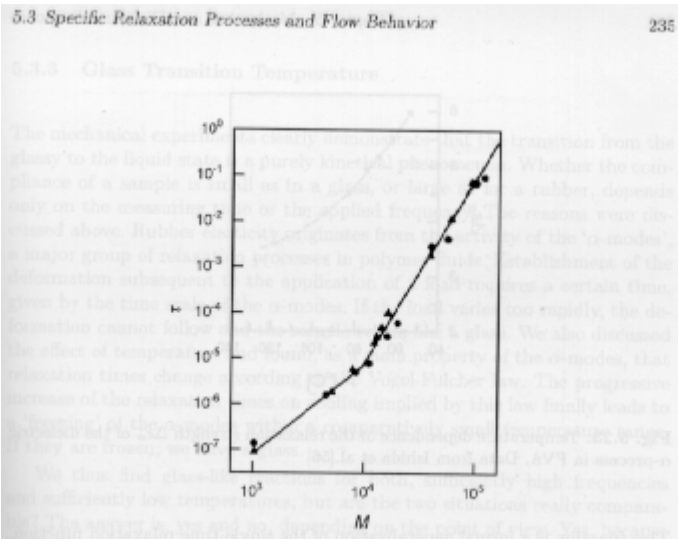

Fig. 5.21. Molecular weight dependence of the relaxation time of the dielectric normal mode in *cis*-PIP. Data from Boese and Kremer [58]

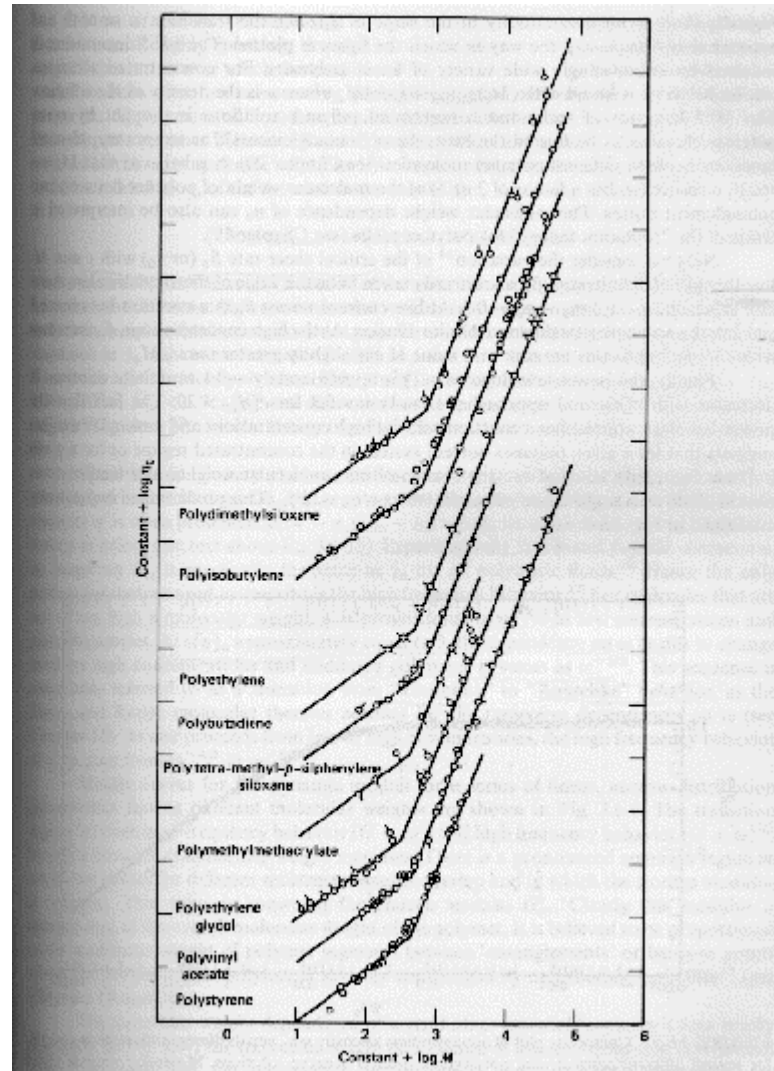

FIGURE 3.6-4. Plots of constant + log η_c vs. constant + log M for nine different polymers. The two constants are different for each of the polymers, and the one appearing in the abscissa is proportional to concentration, which is constant for a given undiluted polymer. For each polymer the slopes of the left and right straight line regions are 1.0 and 3.4, respectively. [G. C. Berry and T. G. Fox, *Adv. Polym. Sci.*, 5, 261–357 (1968).]

Predicts that the viscosity will follow N which is true for low molecular weights in the melt and for fully draining polymers in solution

Rouse model predicts
Relaxation time follows N^2 (actually follows N^3/df)

Hierarchy of Entangled Melts

Hierarchy of Entangled Melts

Chain dynamics in the melt can be described by a small set of "physically motivated, material-specific paramters"

Tube Diameter d_T
Kuhn Length l_K
Packing Length p

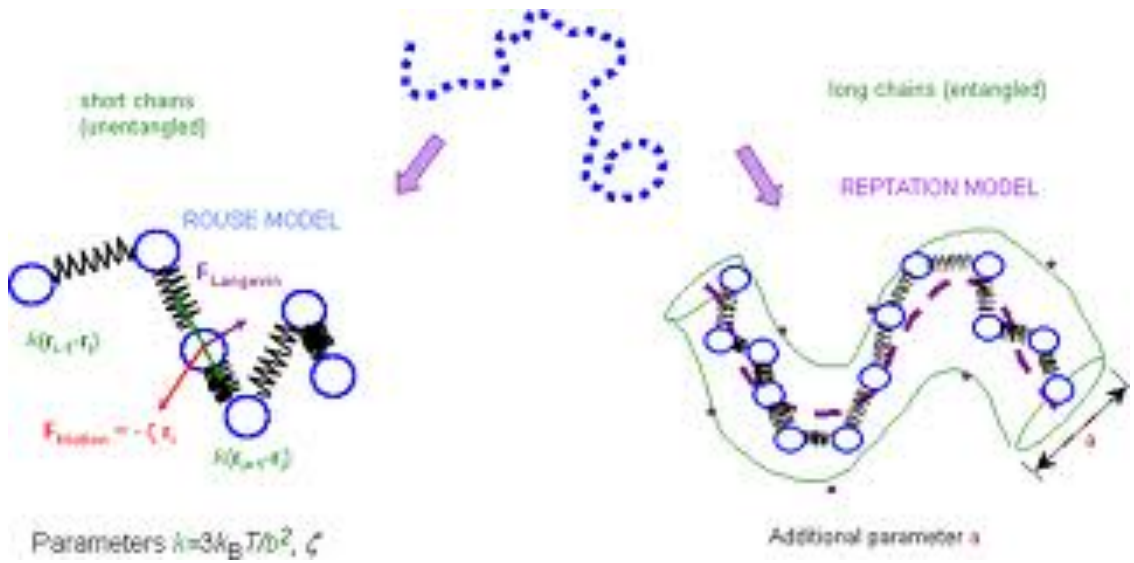

http://www.eng.uc.edu/~gbeaucag/Classes/MorphologyofComplexMaterials/SukumaranScience.pdf

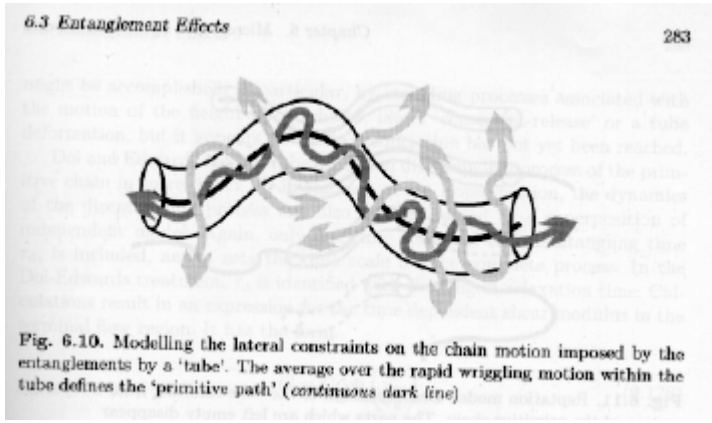

Fig. 6.10. Modelling the lateral constraints on the chain motion imposed by the entanglements by a 'tube'. The average over the rapid wriggling motion within the tube defines the 'primitive path' (*continuous dark line*)

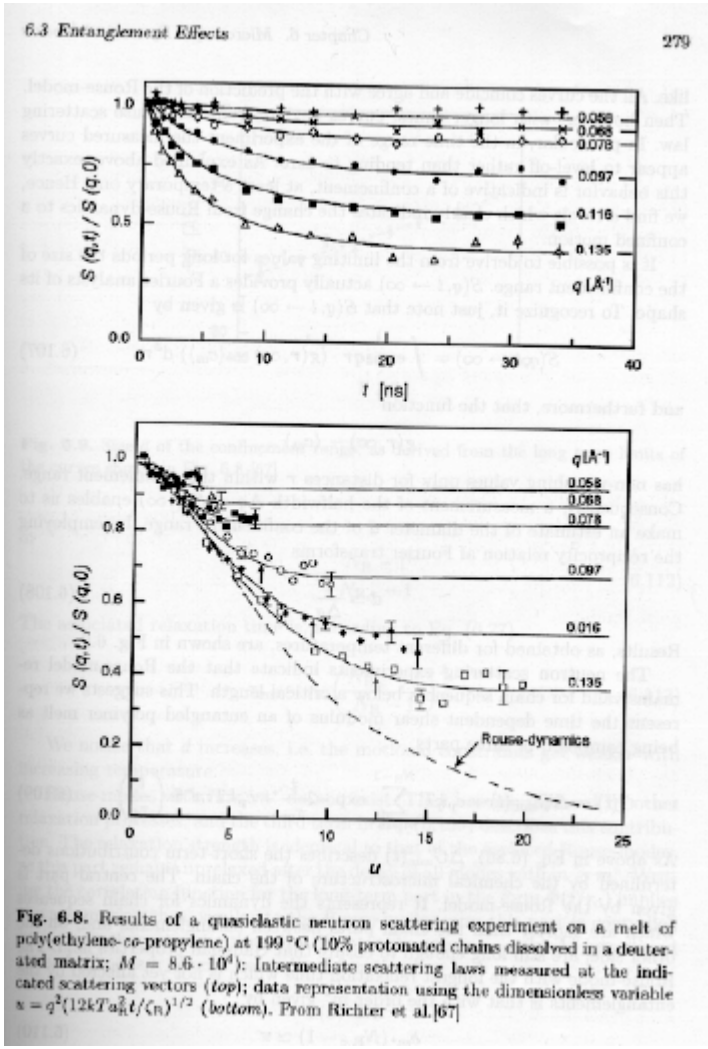

Fig. 6.8. Results of a quasielastic neutron scattering experiment on a melt of poly(ethylene-*co*-propylene) at 199 °C (10% protonated chains dissolved in a deuterated matrix; $M = 8.6 \cdot 10^4$): Intermediate scattering laws measured at the indicated scattering vectors (*top*); data representation using the dimensionless variable $u = q^2(12kTa_R^2 t/\zeta_R)^{1/2}$ (*bottom*). From Richter et al.[67]

Quasi-elastic neutron scattering data
demonstrating the existence of the tube

Unconstrained motion => S(q) goes to 0 at very long times

Each curve is for a different q = 1/size

At small size there are less constraints (within the tube)

At large sizes there is substantial constraint (the tube)

By extrapolation to high times
a size for the tube can be obtained
d_T

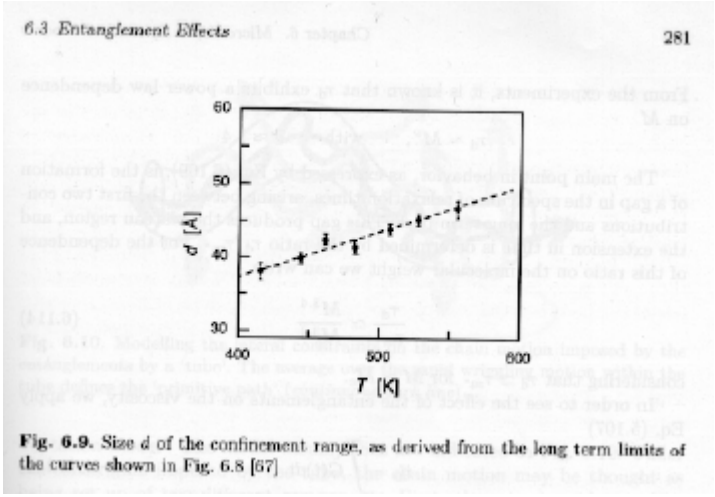

Fig. 6.9. Size d of the confinement range, as derived from the long term limits of the curves shown in Fig. 6.8 [67]

There are two regimes of hierarchy in time dependence
Small-scale unconstrained Rouse behavior
Large-scale tube behavior

We say that the tube follows a "primitive path"
This path can "relax" in time = Tube relaxation or Tube Renewal

Without tube renewal the Reptation model predicts that viscosity follows N^3 (observed is $N^{3.4}$)

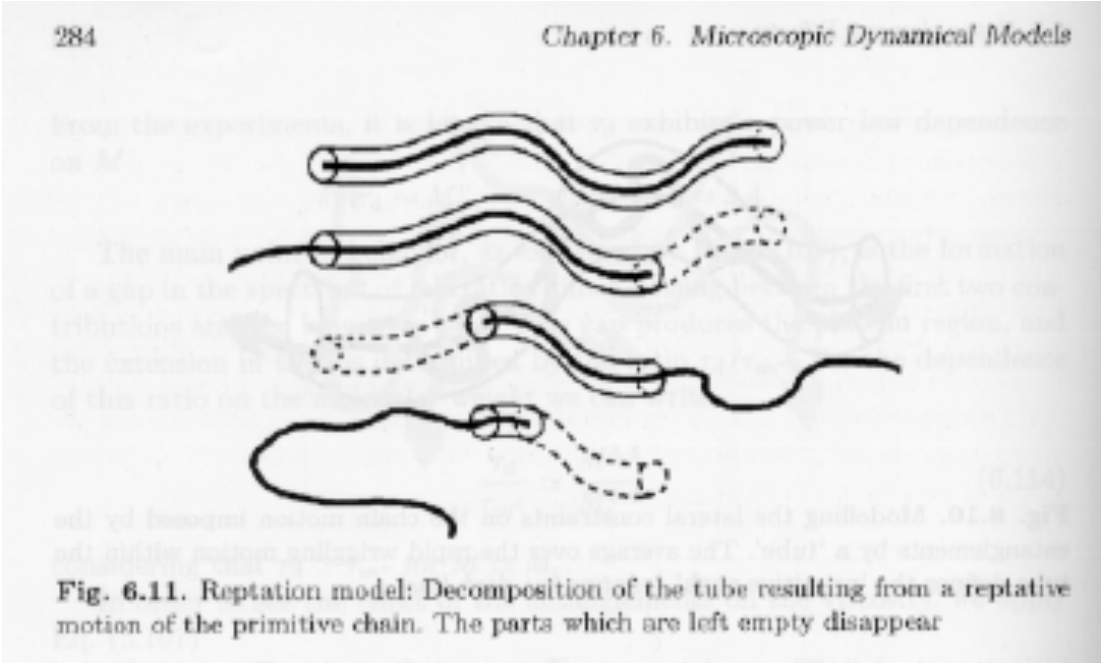

Fig. 6.11. Reptation model: Decomposition of the tube resulting from a reptative motion of the primitive chain. The parts which are left empty disappear

Without tube renewal the Reptation model predicts that viscosity follows N^3 (observed is $N^{3.4}$)

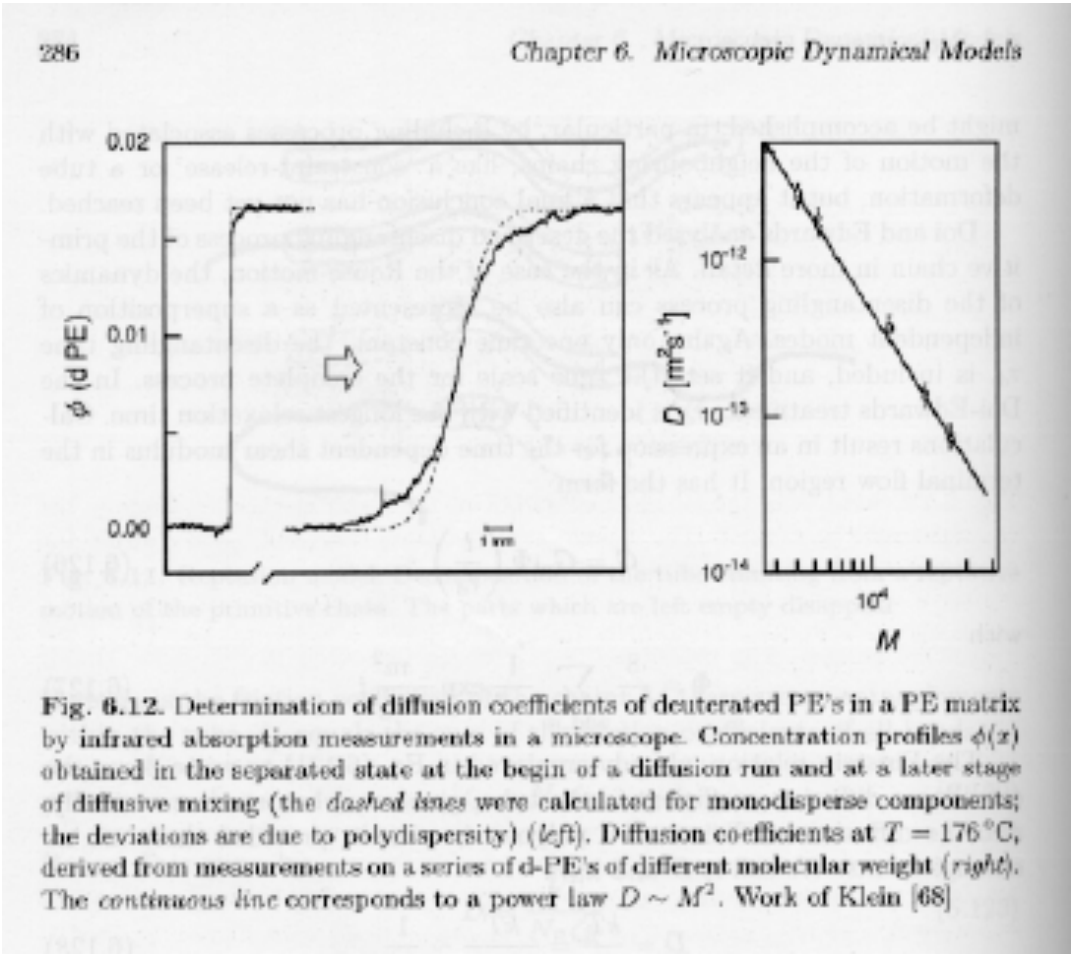

Fig. 6.12. Determination of diffusion coefficients of deuterated PE's in a PE matrix by infrared absorption measurements in a microscope. Concentration profiles $\phi(x)$ obtained in the separated state at the begin of a diffusion run and at a later stage of diffusive mixing (the *dashed lines* were calculated for monodisperse components; the deviations are due to polydispersity) (*left*). Diffusion coefficients at $T = 176\,^{\circ}\mathrm{C}$, derived from measurements on a series of d-PE's of different molecular weight (*right*). The *continuous line* corresponds to a power law $D \sim M^2$. Work of Klein [68]

Reptation predicts that the diffusion coefficient will follow N^2 (Experimentally it follows N^2)
Reptation has some experimental verification
Where it is not verified we understand that tube renewal is the main issue.

(Rouse Model predicts D ~ 1/N)

Reptation of DNA in a concentrated solution

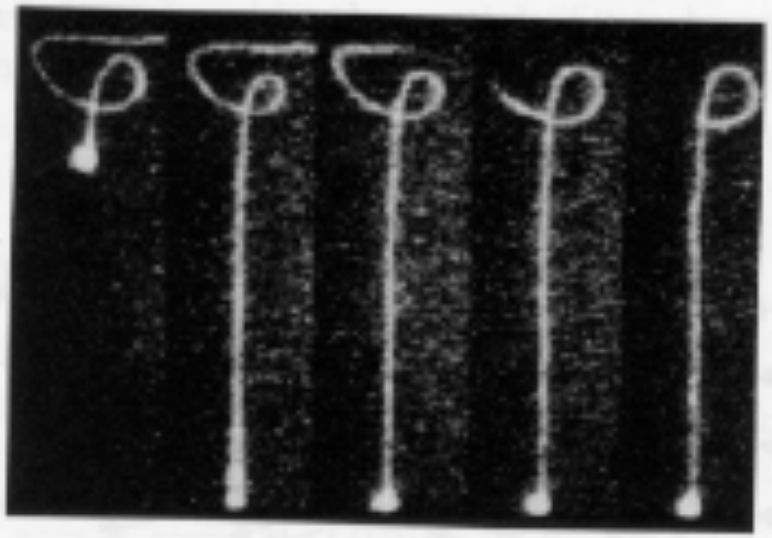

Fig. 6.13. Series of images of a fluorescently stained DNA chain embedded in a concentrated solution of unstained chains: Initial conformation (*left*); partial stretching by a rapid move of the bead at one end (*second from the left*); chain recoil by a reptative motion in the tube (*subsequent pictures to the right*). Reprinted with permission from T.Perkins, D.E.Smith and S.Chu. *Science*, 264:819, 1994. Copyright (1994) American Association for the Advancement of Science

Simulation of the tube

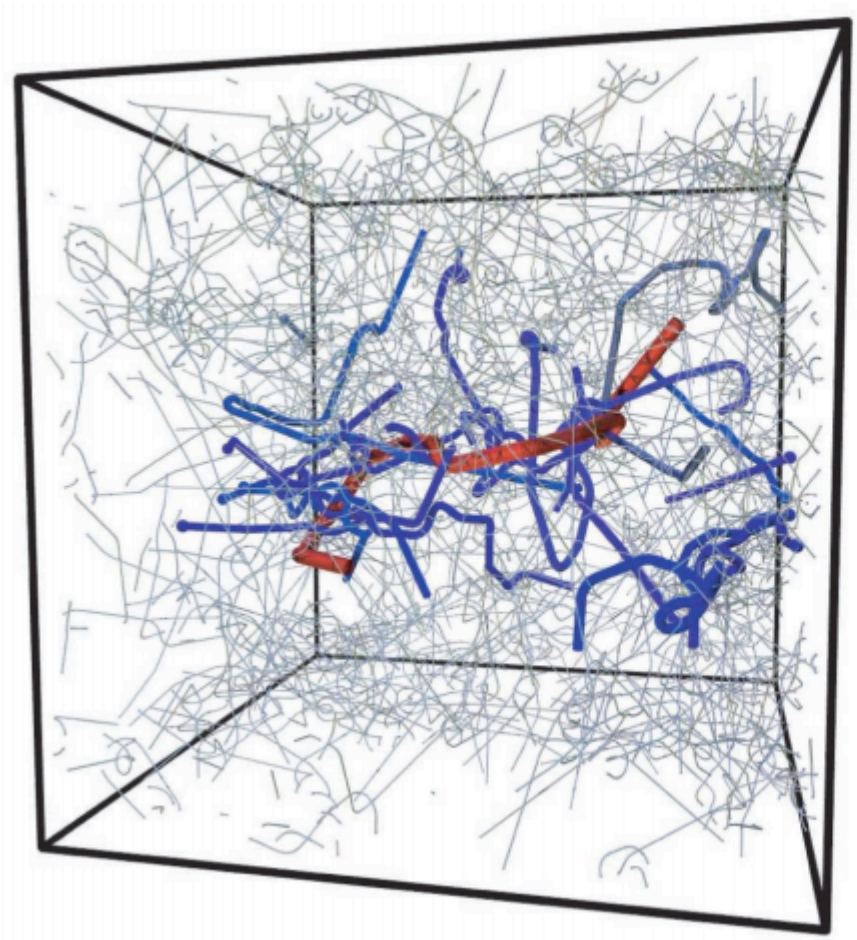

Fig. 3. Result of the primitive-path analysis of a melt of 200 chains of $N + 1 = 350$ beads. We show the primitive path of one chain (red) together with all of those it is entangled with (blue). The primitive paths of all other chains in the system are shown as thin lines.

Simulation of the tube

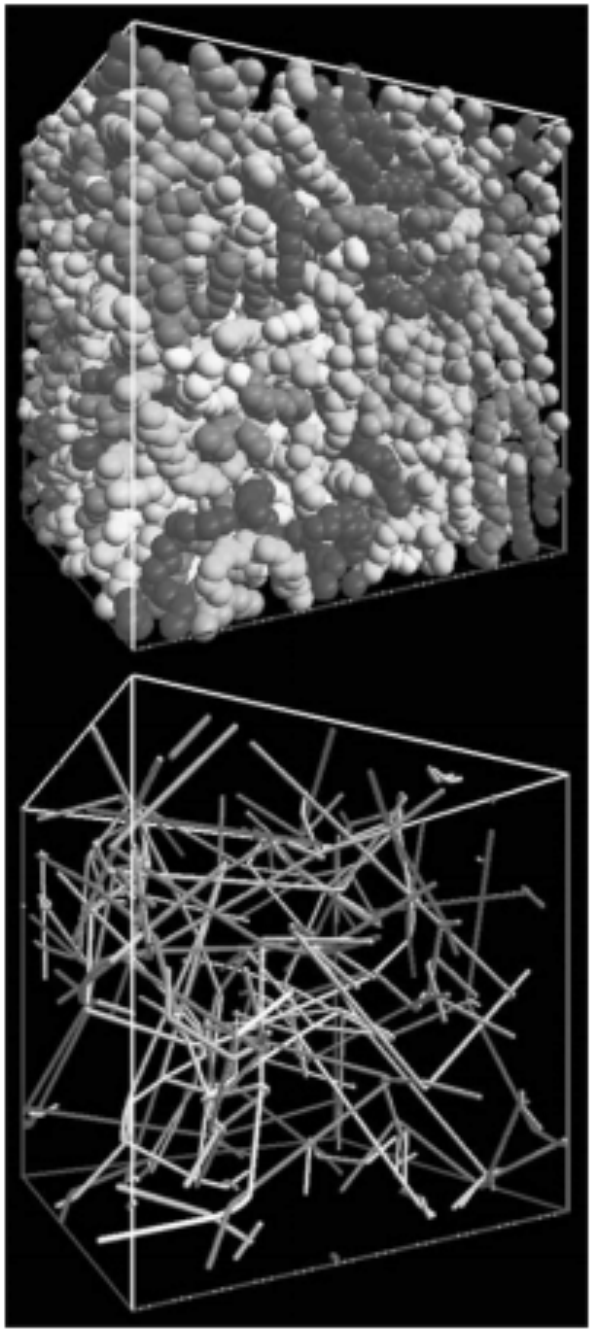

Fig. 3. A representative amorphous polymer sample and the corresponding network of primitive paths.

Plateau Modulus

Not Dependent on N, Depends on T and concentration

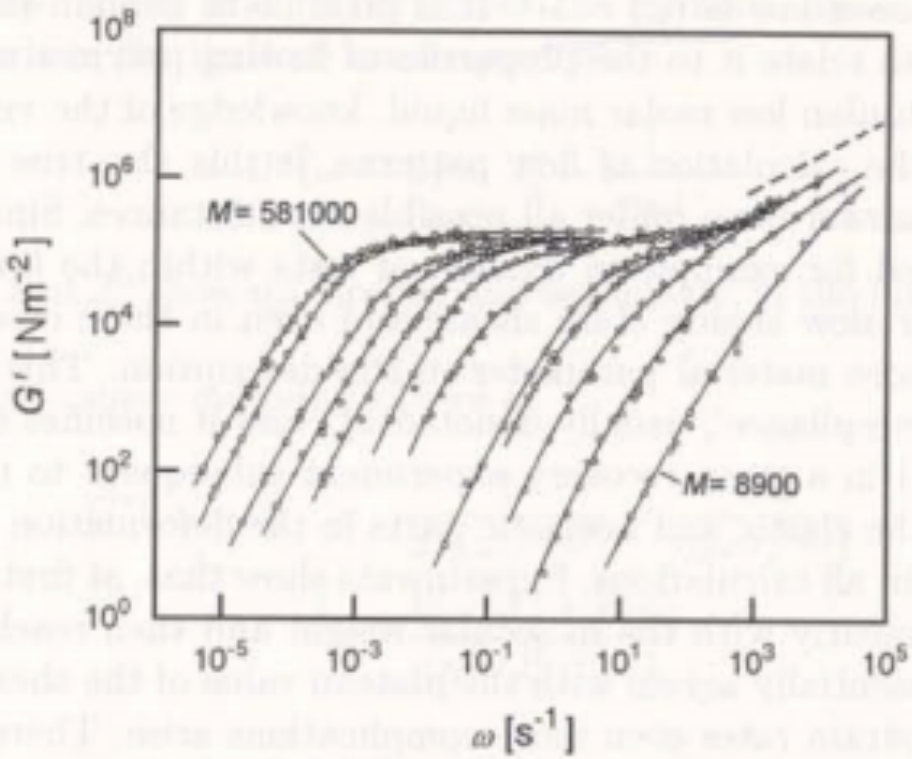

Fig. 5.15. Storage shear moduli measured for a series of fractions of PS with different molecular weights in the range $M = 8.9 \cdot 10^3$ to $M = 5.81 \cdot 10^5$. The *dashed line* in the upper right corner indicates the slope corresponding to the power law Eq. (6.81) derived for the Rouse-model of the glass-transition. Data from Onogi et al.[54]

$$G_0 = \frac{4\rho RT}{5M_e} = \frac{4RT}{5p^3}$$

Kuhn Length- conformations of chains $\langle R^2 \rangle = l_K L$

Packing Length- length were polymers interpenetrate $p = 1/(\rho_{chain} \langle R^2 \rangle)$
where ρ_{chain} is the number density of monomers

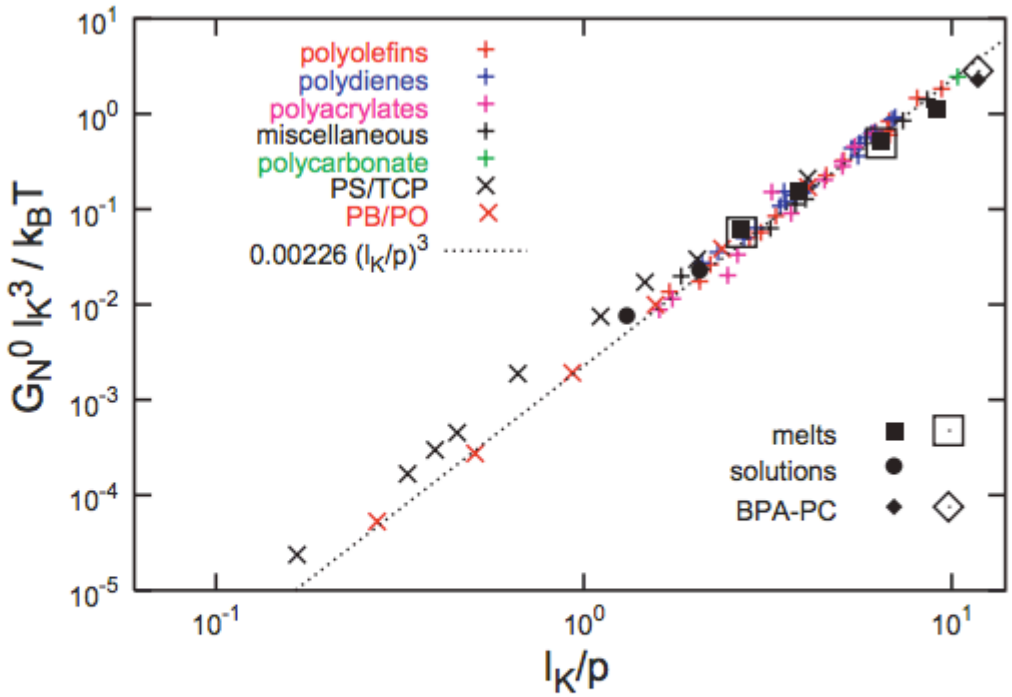

Fig. 2. Dimensionless plateau moduli Gl_K^3/k_BT as a function of the dimensionless ratio l_K/p of Kuhn length l_K and packing length p. The figure contains (i) experimentally measured plateau moduli for polymer melts (*25*) (+; colors mark different groups of polymers as indicated) and semidilute solutions (*26–28*) (×); (ii) plateau moduli inferred from the normal tensions measured in computer simulation of bead-spring melts (*35, 36*) (□) and a semi-atomistic polycarbonate melt (*37*) (◇) under an elongational strain; and (iii) predictions of the tube model Eq. 1 based on the results of our primitive-path analysis for bead-spring melts (■), bead-spring semidilute solutions (●), and the semi-atomistic polycarbonate melt (◆). The line indicates the best fit to the experimental data for polymer melts by Fetters *et al.* (*24*). Errors for all the simulation data are smaller than the symbol size.

this implies that $d_T \sim p$

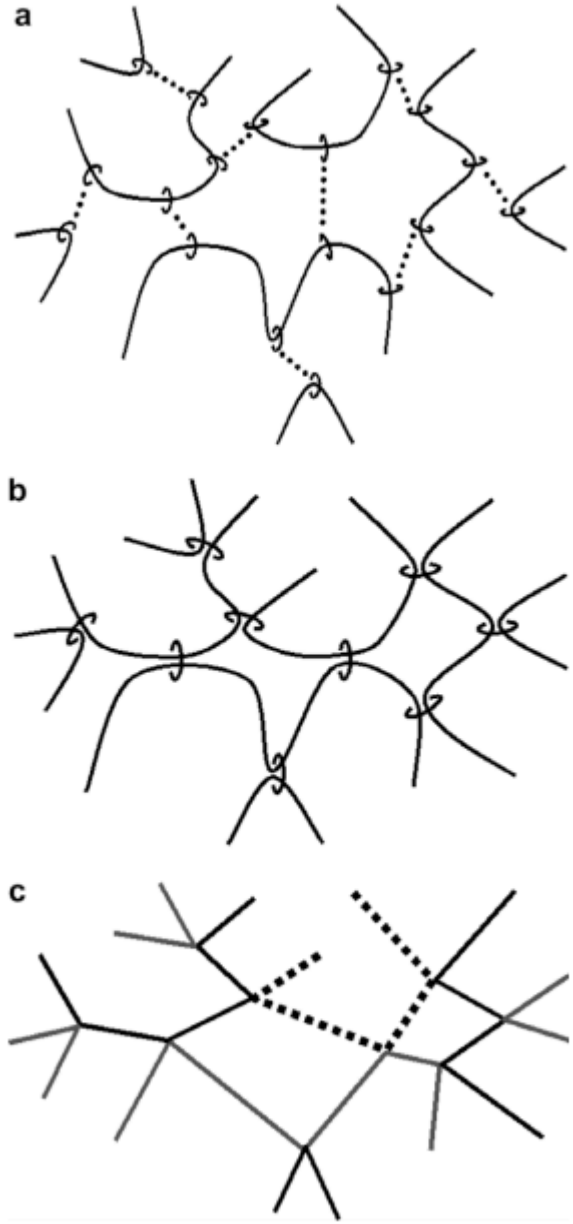

Fig. 1. Schematic representation of dual slip-links. (a) Chains coupled by virtual links. (b) Dual slip-links. (c) Real space representation of the corresponding network of primitive paths.

McLeish/Milner/Read/Larsen Hierarchical Relaxation Model

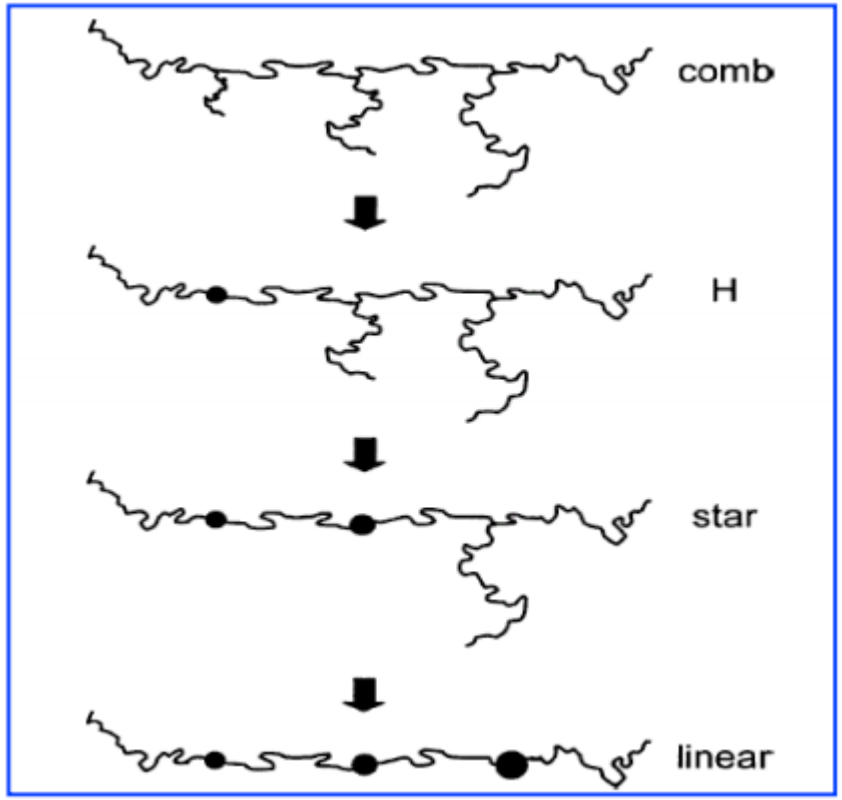

http://www.engin.umich.edu/dept/che/research/larson/downloads/Hierarchical-3.0-manual.pdf